

# Aerosol as a climate-forming component of the atmosphere

## Part 1. Physical properties and chemical composition

K.Ya. Kondratyev

*Center for Ecological Safety RAS/Nansen Environmental and Remote Sensing Center, St. Petersburg*

Received September 17, 2001

Recent studies of physical properties and chemical composition of atmospheric aerosol are reviewed in the context of investigating aerosol as a climate-forming component of the atmosphere with the emphasis on discussion of Aerosol Characterization Experiment (ACE) results. Basic processes responsible for formation of atmospheric aerosol are briefly analyzed. The results of new efforts to justify atmospheric aerosol models are summarized. Major problems in numerical simulation of the spatiotemporal three-dimensional variability of aerosol number density and size distribution are characterized.

### Introduction

Recognizing the problem of potential global climate change, the World Meteorological Organization (WMO) and the United Nations Environment Programme (UNEP) established the Intergovernmental Panel on Climate Change (IPCC) in 1988. The role of the IPCC is to assess the scientific, technical, and socio-economic information relevant for understanding the risks of human-induced climate change. It bases its assessment mainly on peer reviewed and published scientific/technical literature. The maximum possible number (hundreds) of specialists was invoked to complete this task. The IPCC has three Working Groups: Working Group I assesses the scientific aspects of the climate system and climate change (co-chairs of WG I are Ding Yihui (China) and Sir John Houghton (UK)); Working Group II addresses the vulnerability of socio-economic and natural systems to climate change, negative and positive consequences of climate change, and options for adapting to it; Working Group III assesses options for limiting greenhouse gas emissions thus mitigating climate change.

The IPCC completed its First Assessment Report (FAR) in 1990. The FAR played an important role in the development of a UN Framework Convention on Climate Change adopted in 1992 at the Second United Nations Conference on Environment and Development held in Rio de Janeiro and entered into force in 1994. It provides the overall policy framework for addressing the climate change issue. The Second Assessment Report (SAR), Climate Change 1995, provided key input to the negotiations, which led to the adoption of the Kyoto Protocol in 1997. The Third Assessment Report (Climate Change 2001) has been published in 2001. In accordance with the IPCC procedures, these reports went through a triple review process. Comments received during scientific technical review from approximately 1000 governmental and expert reviewers were carefully

analyzed and assimilated to revise the drafts with guidance provided by Review Editors.

Each report included the summary for policymakers (SPM) agreed with representatives of more than 100 countries and representing the statement of the IPCC concerning key findings and uncertainties contained in the Working Group contributions to the reports. Sir John Houghton outlined the main findings in the TAR,<sup>36,39</sup> the principal attention in which was paid to such problems as radiative forcing (RF) due to the increasing atmospheric concentration of greenhouse gases (GHG) and the RF effect on the global circulation of the atmosphere and ocean taking into account that the most probable and significant consequences of the climate warming are the rise of the sea level and intensification of global hydrological cycle.

As to the radiative forcing (defined as a change in the radiation balance of the surface-atmosphere system due to the factors causing climate warming), it is not difficult to estimate its part caused by the change in the GHG concentration. The situation is reversed as applied to estimation of the aerosol RF, especially, its indirect component reflecting the effect of atmospheric aerosol on the properties of cloudiness.<sup>45,48</sup> According to the SAR, the values of shortwave RF for the period since 1850 vary within the limits from 0.1 to 0.5 W/m<sup>2</sup> (the level of the greenhouse effect for this period is 2.4 W/m<sup>2</sup> and, thus, the GHG effect prevails). As to the causes of global climate change in the 20th century (usually, the century-long behavior of the annual global mean surface air temperature (SAT) is considered), the results of numerical simulation of the climate show the following: in spite of the internal variability of the climatic system, the effect of such factors as the increase in the concentration of GHG and anthropogenic aerosol, volcanic eruptions, and extraterrestrial insolation is beyond questions.

A very important aspect of the problem is revealing anthropogenically caused climate changes. The SAR

conclusion that the balance of evidence, from changes in global mean surface air temperature and from changes in geographical, seasonal, and vertical patterns of atmospheric temperature, suggests a discernible human influence on global climate found, in Sir John Houghton's opinion,<sup>36</sup> even more cogent confirmation. The particular attention in recent was paid to the problem of global carbon cycle in the context of biospheric effect on it, since it is still unclear whether the global biosphere is a carbon source or sink and, moreover, whether the changes in the carbon cycle will be still difficult-to-predict in the future.<sup>12,47</sup> On the average for the globe, the vegetation cover in the 1980's was the source of carbon, but in the 1990's the opposite tendency, i.e., vegetation cover functioning as a CO<sub>2</sub> sink, appeared. This situation will likely hold as applied to the land biosphere in the first part of the 21st century, but later it may transform into the carbon source.

Considerable progress is achieved in improvement of numerical models of the global climate, especially, from the viewpoint of the allowance for the atmosphere-ocean interaction, what permitted eliminating (in many models) the use of the so-called flux correction. Serious progress is also achieved in numerical simulation of regional climate as applied, for example, to analysis of the possible effect of global warming on such phenomena as El Niño/Southern Oscillation and on thermohaline circulation (paleoclimatic data evidence that in the past the latter was destroyed several times).

Starting from the fact that in the 21st century the climate will possibly change faster than for the last 10 000 years, we arrive, in particular, at two important conclusions associated with global warming: (1) destructive consequences (for many countries) from the rise of the sea level and (2) considerable changes in the global hydrological cycle, which can be accompanied by both floods and droughts. In accordance with Article 3 of United Nations Framework Convention on Climate Changes, "...The Parties should take precautionary measures to anticipate, prevent or minimize the causes of climate change and mitigate its adverse effects. Where there are threats of serious or irreversible damage, lack of full scientific certainty should not be used as a reason for postponing such measures, taking into account that policies and measures to deal with climate change should be cost-effective so as to ensure global benefits at the lowest possible cost. At the same time, in accordance with Article 2, "The ultimate objective of this Convention ... is to achieve ... stabilization of greenhouse gas concentrations in the atmosphere at a level that would prevent dangerous anthropogenic interference with the climate system. Such a level should be achieved within a time-frame sufficient to allow ecosystems to adapt naturally to climate change, to ensure that food production is not threatened and to enable economic development to proceed in a sustainable manner. In the opinion of the World Energy Council (WEC), the most important goal of developed countries is to reduce CO<sub>2</sub> emissions by about 30% by 2020. This will require expenses of about 1% of the global gross production.

In the context of acute discussions on the Kyoto Protocol,<sup>9</sup> in particular, at the G-8 Summit in Genoa in July 2001, the particular attention is paid to a high degree of uncertainty in estimates of the anthropogenic effect on the global climate. One of the main uncertainties is connected with the absence of adequate information on the global space-time variability in the concentration of different-type aerosol, physical (especially, optical) properties of aerosol, and its effect on the microphysical processes in clouds. These circumstances seriously complicate assessment of the climatic effect of the atmospheric aerosol. The goal of the first part of this review is to discuss the information concerning physical properties and chemical composition of atmospheric aerosol. It should be noted that this issue is considered in TAR Chapter 5, which is cited below. Unfortunately, the authors of this Chapter<sup>39</sup> ignored the results obtained by Russian scientists (in spite of my suggestions), as well as many other important results. Just these facts stimulated the appearance of this review, taking into account that many problems forming its subject were discussed earlier.<sup>13,82</sup>

## 1. Production and properties of atmospheric aerosol

Atmospheric aerosol is a product of complex combination of chemical and physical processes. Because of the complexity of these processes and relatively short lifetime, the chemical composition and physical characteristics of aerosol vary widely. The space-time variability of aerosol characteristics is so wide and observations are so fragmentary, that reliable estimates of the global budget of aerosol from various sources are still impossible and available estimates of the emission rates of global sources of natural and anthropogenic aerosol are only approximate.

However, there is no question that assessments of anthropogenic aerosol are more reliable than those of natural aerosol (especially, in hard-to-reach regions of the World Ocean and continents). This situation determines low reliability of data on the proportion between natural and anthropogenic aerosol, though the effect of human activity on the nitrogen and sulfur cycles is undoubted.

Classification of the atmospheric aerosol in accordance with its sources distinguishes the following types of natural aerosol: (1) products of evaporation of sea spray; (2) mineral dust uplifted by wind into the atmosphere; (3) volcanic aerosol (both directly emitted into the atmosphere and generated in gas-phase reactions); (4) particles of biogenic origin (directly emitted into the atmosphere and produced due to condensation of volatile organic compounds, for example, terpenes, as well as chemical reactions between them); (5) smoke produced from burning of land biota; (6) products of gas-phase reactions (for example, sulfates produced due to reduction of sulfur coming from the ocean surface as emissions of dimethylsulfide<sup>47,48</sup>).

The most important anthropogenic aerosols are: (1) direct industrial emissions of particles (soot, smoke, dust, etc.) and (2) products of gas-phase reactions.

Besides, it is worth distinguishing the tropospheric and stratospheric (mostly volcanic) aerosol.

Of great interest are gas-phase reactions producing aerosol due to the following processes: (1) homogeneous homomolecular nucleation (gas-phase production of new stable liquid or solid fine particles with participation of only one gas component); (2) homogeneous heteromolecular nucleation (similar process, but with participation of two or more gases); (3) heterogeneous heteromolecular condensation (growth of already existing particles due to gas adsorption).

According to Ref. 39, the following primary and secondary sources of aerosol should be distinguished: soil dust, sea salts, industrial dust, and primary anthropogenic aerosol (organic and black carbon), primary biogenic aerosol, sulfates, nitrates, and volcanic aerosol.

Photochemical and chemical reactions responsible for primary transformation of the highly volatile gas into the gas component that are initial for aerosol formation are very complex and poorly studied yet. The most significant parts are likely played by the following processes: (1) reaction of sulfur dioxide with hydroxyl radicals, which finally leads to generation of sulfuric acid molecules and sulfuric acid aerosol; (2) reactions of non-methane hydrocarbons with ozone and/or hydroxyl radicals with production of aldehydes, alcohols, carboxylic and dicarboxylic acids (as a rule, secondary products of these reactions react with nitrogen oxides, what leads to production of organic nitrates).

Ozone and hydroxyl radicals ( $\text{HO}$  and  $\text{HO}_2$ ), which are direct or indirect products of chemical reactions (just therefore the processes of gas-phase production of particles are characterized by pronounced diurnal behavior), usually play a very important part in atmospheric chemistry.

Particles of organic compounds are among the most important types of atmospheric aerosol.<sup>8</sup> Various organic compounds take part in the so large number of reactions that the study of organic aerosol is extraordinarily difficult. The atmospheric concentration of soot particles is also very significant, achieving the mean values about  $0.5 \mu\text{g}/\text{m}^3$  over oceans; it is comparable with the concentration of mineral dust aerosol. The global organic aerosol likely originates to the equal extent from both natural and anthropogenic sources, and the ocean is responsible for about a half of natural aerosol.

The results of aerosol effect on different processes (for example, radiative transfer) depend, as a rule, on the combination of chemical and physical processes, and the dependence of the aerosol composition on the particle size spectrum almost always plays a significant part. Therefore, adequate description of the properties of actual aerosol is only possible by use of the results of combined determination of its characteristics. One of the most widely used types of aerosol measurements is determination of its mass concentration, but just this characteristic is the least informative, because it says

nothing about the sources and composition of aerosol, as well as its possible effects.

Aerosol cycles are closely connected with hydrological processes in the atmosphere because of significant interaction between aerosol and clouds: clouds and precipitation play a significant part in the production, transformation, and removal of aerosol from the atmosphere, but, on the other hand, aerosol significantly affects microphysical processes in clouds. It is not an accident that in most regions of the globe the aerosol lifetime in the lower and upper troposphere is 1-2 weeks, and for water vapor the lifetime is 10 days. The connection between clouds and aerosol indicates that it is impossible to thoroughly understand aerosol production and transformation processes without reliable knowledge of cloud physics and chemistry. In this connection, the study of nucleation mechanisms is of crucial importance.

The apprehension concerning the possible anthropogenic increase in the aerosol content is quite reasonable, since it may affect climate both through the changes in the Earth's radiative balance and by affecting the hydrological cycle. However, the wide space-time variability of aerosol characteristics complicates separation of its anthropogenic component. It can be separated only when we understand thoroughly the causes of this variability, what requires wide combined investigations of atmospheric aerosol.

Many-year studies of the atmospheric aerosol within the framework of CAENEX and GAREX<sup>6,7,48</sup> were followed by numerous new investigations. The main goal of this review is just the discussion of these new results.

### 1.1. Aerosol Characterization Experiment (ACE)

The Program of the ACE-1 Southern Hemisphere Aerosol Characterization Experiment was developed to obtain more reliable information about aerosol and refine the estimates of its effect on climate within the framework of the International Global Atmospheric Chemistry (IGAC) Project – a core project of the International Geosphere-Biosphere Programme (IGBP). The ACE-1 was aimed at studying chemical and physical processes determining the properties of marine aerosol in the Southern Hemisphere and estimation of its effect on climate.<sup>17,18</sup> This required further development of global aerosol transport models taking into account its chemical transformation and application of the radiative transfer theory under conditions of cloudless and cloudy atmosphere for calculation of radiative fluxes and heat flux divergences needed for analysis of aerosol interaction with various components of the climate system.

Another important goal was to obtain adequate information about such characteristics determining the aerosol effect on radiative transfer as light scattering efficiency per unit mass  $\alpha_{\text{sp}}$ , fraction of backscattered radiation  $\beta$ , asymmetry factor of the scattering phase functions  $g$ , single scattering albedo  $\omega_0$ , and dependence of aerosol scattering on relative humidity  $f_{\text{sp}}(\text{RH})$ . All these characteristics depend on the chemical composition,

size distribution, morphology, and other properties of aerosol. Because of the considerable role of aerosol of gas-phase origin, the information about its gaseous precursors is of great importance.

The reliable information about the aerosol effect on climate can be obtained only through execution of a combined program of observations under both field and laboratory conditions along with numerical simulation. The ACE was planned to include field observations in various representative regions of the globe. The main ACE objectives were (1) to obtain the data on physical and chemical properties of the main types of aerosol (as well as relationships between these aerosol properties), including the aerosol characteristics determining the aerosol effect on the formation of clouds (nucleation properties); (2) to study physical and chemical processes controlling formation and evolution of the main types of aerosol and the properties determining the aerosol microstructure, chemical composition, radiative and nucleation characteristics; (3) to check the reliability of various aerosol parameterization schemes in regional and global climate models.

The ACE-1, the first in the series of field experiments studying physical, chemical, and nucleation properties of atmospheric aerosol, was conducted in the period from November 15 to December 14 of 1995 over the southwestern sector of the Pacific Ocean (to the south from Australia).<sup>18</sup> The ACE-1 involved 47 research groups from 11 countries and included coordinated measurements from the NCAR C-130 aircraft, the NOAA research vessel *Discoverer*, the Australia fisheries research vessel *Southern Surveyor*, and land based stations at Cape Grim and Macquarie Island, Australia.

Keeping in mind the particular role of dimethylsulfide emitted into the atmosphere from the ocean, scientists studied characteristics of four water masses in the region of ACE-1 in order to analyze the effect of their chemical and biological properties on the content of various trace constituents. In this connection, it is important that the ocean is a source of such biogenic substances in the atmosphere, as dimethylsulfide (DMS), hydrocarbons, methyl nitrates, and methyl halides.<sup>8</sup> The ocean can also be a source of biogenic calcium carbonate which favors the increase in alkalinity of the sea-salt aerosol and ozone-induced oxidation of sulfur dioxide being a part of aerosol water.

The data published earlier indicate that the dominant aerosol component in the region under consideration is the sea-salt aerosol (this refers to 90% of particles >130 nm in diameter and 70% of particles > 80 nm in diameter). Organic components relevant to sea salt are found in 50% of aerosol particles >160 nm in diameter. These facts show that the sea-salt aerosol should necessarily be taken into account in climate models, since it controls not only the scattering of solar radiation, but also the concentration of cloud condensation nuclei.

The results discussed by Bates in Refs. 17 and 18 showed that the anthropogenic effect on the atmosphere and the aerosol properties is still pronounced even in

remote ocean regions. Thus, for example, layers containing aged biomass burning products were observed at the altitude above 3 km. About 11–46% of sulfate aerosol particles >100 nm in diameter contained soot, which probably originated from biomass burning in South America.

The ACE-1 data allows estimation of the role of biogenic components in formation and growth of new aerosol particles. Photochemical production of new particles from sulfuric acid in the areas of emissions from clouds was observed as well. The results of numerical simulation indicate that about 30–50% of DMS is transformed into SO<sub>2</sub>, and the main sink for sulfur dioxide is its ozone-induced oxidation in aerosol water. Non-sea-salt sulfates were mostly contained in super-micrometer sea-salt particles, making up to (35±10)% in summer and (58±22)% in winter.

## 1.2. Background marine aerosol

The atmosphere in remote regions of the World Ocean is a chemically dynamic system, which, in particular, involves production of the sea-salt aerosol (due to destruction of droplets coming to the atmosphere from the sea surface) and the non-sea-salt (NSS) aerosol as a product of gas-phase reactions of transformation of biogenic dimethylsulfide emitted into the atmosphere from the ocean. To check numerous hypotheses concerning the sources and properties of the background marine aerosol, Huebert et al.<sup>38</sup> have analyzed airborne measurements of the NSS concentration, as well as the concentrations of methanesulfonate (MS) anions and cations, ammonium, potassium, nitrate, and other gaseous components obtained during ACE-1 with the results of ground-based measurements at Cape Grim.

Processing of the observations revealed the presence of high gradient in the MS concentration in the free troposphere of the Southern Hemisphere in spring, whereas for NSS this gradient was absent. The major part of the studied components was characterized by the pronounced vertical gradients of the concentration with the values near biogenic sources in the atmospheric boundary layer higher than those in the free atmosphere. The data of Lagrangian experiments and observations at Cape Grim revealed the presence of photochemically caused MS formation in daytime at the unchanged or decreasing MS concentration during nighttime. The NSS concentration grew in daytime as well. The MS/NSS concentration ratio was characterized by the highest latitude gradient with the values measured in the most southern point close to those measured in the snow cover of Antarctic Plateau.

Although the formation of finest aerosol particles (nucleation) in the unpolluted marine boundary layer is of great importance (especially, from the viewpoint of the effect of such particles on the cloud properties), the observations of the nucleation process are still few and fragmentary. In this connection, O'Dowd et al.<sup>59,60</sup> observed several nucleation events (formation of ultrafine aerosol particles) at Mace Head on the west coast of

Ireland in 1996 using two condensation nuclei (CN) counters measuring the number density of particles with the radii  $>1.5$  and  $>5$  nm. The difference between the counters' readings gives the number density of particles with the radii from 1.5 to 5 nm.

The concentration of soot carbon was measured simultaneously, and the results of these measurements demonstrated the presence (in two cases) of clean air with the soot carbon concentration less than  $20 \text{ ng/m}^3$ . Besides, the radon concentration was measured (for estimation of the possible yield of the continental aerosol, which turned out insignificant, because the radon concentration was lower than 0.4 or  $0.8 \text{ pCi/m}^3$ , what is typical of the marine air mass in North Atlantic).

Nucleation events occurred often and had the space scale from tens to hundreds of meters and the time scale from seconds to minutes under two conditions: (1) low tide and (2) rather intense solar radiation. The first of these conditions determines the presence of open sea bottom, which is the source of gaseous CN precursors. It is assumed that volatile organic compounds and/or alkylhalide derivatives served such precursors. As to the solar radiation, it stimulates photochemical production of new particles (nucleation was not observed at nighttime). The nucleation rate was estimated as  $10^3\text{--}10^4 \text{ cm}^{-3} \cdot \text{s}^{-1}$ , thus indicating that the coastal zone is a significant source of atmospheric condensation nuclei.

The studies of the marine boundary layer showed that atmospheric aerosol, especially, particulates that serve cloud condensation nuclei (CCN), not only affects clouds (changing their structure and optical properties), but also experiences the back effect of the cloud medium, which changes the particulate concentration and other characteristics. This effect can be represented by different mechanisms.<sup>28</sup>

First of all, some evidence indicates that the nucleation process proceeds just under the cloud top. This process is responsible for the high concentration of sulfate particles produced likely due to heteromolecular nucleation in the regions with high relative humidity. This leads to the growth in the number density of aerosol particles, which can finally play the key role as CCN, achieving a sufficient size.

Another possible mechanism is the increase of the droplet mass due to various chemical reactions in the aqueous phase. Complete evaporation of such droplets produces aerosol particulates, which can serve CCN. An important circumstance is that in the latter case the particulate mass concentration increases, while the number density does not increase. Thus, CCN become larger and can be activated more easily (as CCN) in the case of supersaturation in the ambient air.

One more possible mechanism is connected with particle collision/coalescence processes. All the three mechanisms mentioned above can manifest themselves to different extent in all clouds. However, no attempts to compare their significance were undertaken yet.

In this connection, using some particular situations as an example, Feingold et al.<sup>28</sup> analyzed the significance of the mechanisms of collision/coalescence and

chemical processes in the aqueous phase. The main goal of this analysis was to study processes occurring in the marine boundary layer (MBL) with 300-m thick stratocumulus clouds in its upper part. This selection of the object for study was motivated by several circumstances: the important MBL contribution to formation of the global radiative budget, assumed sensitivity of MBL cloudiness to the CCN concentration, the low, as a rule, CCN concentration in the considered situation, what favors strengthening of the effect of processes in clouds on CCN.

The results obtained in Ref. 28 are based on the use of a 2D version of regional vertex resolving model of atmospheric processes developed in the University of Colorado (USA) and already applied to study stratocumulus dynamics. The effect of collision/coalescence processes leading to the decrease of the number density of droplets and, thus, CCN was simulated numerically neglecting wet scavenging, and the obtained results were compared with the data characterizing the role of chemical processes in the aqueous phase. Such microphysical processes as activation of droplets, condensation (evaporation, collision), coalescence, deposition, and regeneration of particles arising at complete droplet evaporation were considered in detail.

The calculations showed that the collision/coalescence processes can lead to a significant decrease in the droplet number density (up to 22% per hour) and this causes a significant growth of the particle radius (about 7% per hour). For a more detailed analysis of the collision/coalescence processes (in particular, the time of particulate sedimentation in clouds) and estimation of the intensity of sulfur dioxide transformation into sulfates in clouds, particulate trajectories were calculated. These calculations have led to the conclusion that both mechanisms studied have a comparable effect on CCN manifesting itself in the growth of particles (under certain conditions).

Evidences for stratocumulus located far from pollution sources indicate that the effect of chemical reactions in the aqueous phase can be stronger at lower water content of lower-level clouds, whereas the collision/coalescence mechanism can dominate in the case of the higher water content or at a wide droplet size spectrum.

In the process of studying the radiative effects of aerosol in the MBL, the contributions of the sea-salt and non-sea-salt components of sulfate aerosol (SA) to such effects were hotly debated. The dominant aerosol in the MBL is that consisting of volatile sulfate particles less than  $0.08 \mu\text{m}$  in size having the highest number density, though the larger part of the aerosol mass is concentrated in much smaller number of sea-salt particles larger than  $1 \mu\text{m}$ . The aerosol-induced radiative forcing of climate is, however, formed due to sub-micrometer particles of intermediate size ( $0.08\text{--}1 \mu\text{m}$ ), because just they scatter the solar radiation most intensely, as well as serve the cloud condensation nuclei. Therefore, it was earlier assumed that the sulfate aerosol produced due to dimethylsulfide emissions from the ocean and the following gas-phase reactions can significantly affect climate through radiative forcing.

Usually it is assumed that marine aerosol particles smaller than  $1\ \mu\text{m}$  consist of sulfates of non-marine origin, but recent investigations has led (though according to indirect evidence) to the conclusion that such particles of the sub-micrometer size contain, at least partially, marine sulfates. In this connection, Murphy et al.<sup>57</sup> discussed the results of direct measurements of the chemical composition of aerosol particles within the framework of the ACE-1 experiment. It follows from these results that almost all particles larger than  $0.13\ \mu\text{m}$  in MBL contained sea salts. Such a marine aerosol was mostly responsible for scattering of the solar radiation and contained a considerable number of cloud condensation nuclei. Aerosol particles usually were an internal mixture of sea salts and sulfates, in which one component can hardly be separated from another. Sub-micrometer particles contained also a small amount of organic components.

Many earlier numerical models of aerosol formation were intended for reconstructing the results of laboratory experiments. At the further stage of their development, they provided for consideration of a multicomponent aerosol with allowance for the processes of gas-phase transformation. These results have formed the basis for box models of the process of aerosol formation in the atmospheric boundary layer. It was just this approach Fitzgerald et al.<sup>30,31</sup> used for numerical simulation of homogeneous nucleation of new particles and their following growth up to the size of cloud condensation nuclei in the marine boundary layer.

Since such models cannot reconstruct changes in the processes of aerosol formation with height, in Ref. 30 a one-dimensional model was proposed. The model provides for reconstruction of changes in the aerosol properties with time and height in MBL. An important feature of the new model is its capability of describing adequately the aerosol transport in the atmosphere in the presence of the humidity gradient. The restrictive circumstance is, however, the assumption on the instantaneous leveling of the water vapor content in particles with respect to the ambient atmosphere, what artificially restricts the maximum size of particles to less than  $30\ \mu\text{m}$  in radius.

The discussed model accounts for all known significant processes determining formation of the microstructure of four-component aerosol (sulfates, sea salts, insoluble continental component, water) in MBL: production of the sea-salt aerosol on the ocean surface, nucleation of new particles, coagulation, condensation growth of particles of gas-phase origin, growth of sulfate particles in the process of their processing by clouds, aerosol scavenging by precipitation, deposition onto the surface, turbulent mixing, gravitational settling and exchange with the free troposphere. It also takes into consideration the processes of gas-phase transformation describing formation of sulfate aerosol due to oxidation of dimethylsulfide (photooxidation of DMS to  $\text{SO}_2$ ) and sulfur dioxide (oxidation of  $\text{SO}_2$  to  $\text{H}_2\text{SO}_4$ ) with the following production of particles (at the given diurnal behavior of the hydroxyl concentration). The proposed model can be implemented as an interactive component

of the meteorological mesoscale three-dimensional model of MBL.

Fitzgerald et al.<sup>31</sup> discussed the results of numerical simulation of aerosol and transformation production processes in the marine boundary layer under conditions of the remote oceanic atmosphere of the Southern Hemisphere (near Tasmania) using the MARBLES one-dimensional model of multicomponent aerosol dynamics in MBL. The main goal of numerical simulation was analysis of processes responsible for the formation of aerosol microstructure through successive consideration of various factors determining it. The principal attention was paid to the interesting processes of aerosol processing by clouds and aerosol exchange between MBL and the free troposphere.

The calculations showed that the transformation of aerosol properties by clouds manifests itself in the appearance of characteristic double maximum of the microstructure in the upper part of MBL and in the characteristic aerosol lifetime at the sea surface level: it is much shorter than the characteristic time corresponding to the interaction with the troposphere (in this case, the typical exchange rate is about  $0.6\ \text{cm/s}$ ). According to the calculations, the free troposphere can be a considerable source of particles for MBL in the size range corresponding to the minimum size of particles processed by clouds, whose growth is determined by the transformation of dissolved  $\text{SO}_2$  into sulfates in cloud droplets. The exchange between MBL and the troposphere contributes markedly to formation of the aerosol microstructure in the MBL.

The considered model was also applied to trace the aerosol evolution in air mass experiencing advection from the East Coast of the USA to the central part of the Atlantic Ocean for periods up to 10 days long. In the process of such advection, transformation of the microstructure from continental to marine (characteristic of remote ocean) takes 6–8 days. Nucleation in the considered case of typical meteorological conditions did not occur, but under less typical conditions, including significant aerosol scavenging (precipitation of  $5\ \text{mm/h}$  for 12 hours), temperature drop by  $10\ \text{K}$  (from  $283\ \text{K}$  near the surface to  $279\ \text{K}$  at the height of  $1000\ \text{m}$ ), and intense DMS flow ( $40\ \mu\text{mol}/(\text{m}^2 \cdot \text{day})$ ), considerable nucleation may occur. The estimated sensitivity of the results to the initial conditions demonstrated that it almost did not manifest itself for the entire period of numerical simulation (8–10 days).

### 1.3. Carbon aerosol

Investigations of carbon aerosol attract particular attention. Production of the anthropogenic component of carbon aerosol in the global atmosphere was estimated to be  $12\text{--}24\ \text{Tg/yr}$ . Therefore, this aerosol has a considerable effect on such processes as light scattering and absorption in the atmosphere and chemical reactions, as well as the human health. Since this effect depends on the level of hydration of carbon aerosol particles, the

problem of interaction of the carbon aerosol with water is quite urgent. It is known, for example, that SO<sub>2</sub> oxidation regulated by soot carbon and the photodegradation of polyaromatic hydrocarbon compounds connected with soot particles depend on the presence of water.

To study further hydration of soot particles, Chugthai et al.<sup>24a</sup> conducted laboratory measurements of the capability of different soot particles (TR-8 fuel for jet airplanes, kerosene, diesel oil, metal and sulfur-containing synthetic substances) to capture water. Drawing of soot adsorption and desorption isotherms (model of *n*-hexane) allowed determination of such a water desorption parameter as the surface cover at the limiting level of chemisorption and the relative humidity equal to 83%. The obtained values increase as the soot surface oxidizes at the relative humidity from 35 to 85%, whereas the hydration level at the lower relative humidity (up to 92%) depends on the fuel composition and conditions of its burning. Soot containing metals and sulfur is characterized by higher hydration level. The obtained results were used to estimate the effect of relative humidity on the kinetics of soot oxidation reactions with participation of O<sub>3</sub>, NO<sub>2</sub>, and other gaseous atmospheric constituents.

Posfai et al.<sup>66</sup> studied aerosol particles containing soot aggregates under conditions of marine atmosphere with air varying from unpolluted to strongly polluted in both hemispheres. The analysis of these observations showed that even in clean atmosphere of a remote region of the Southern Hemisphere from 10 to 45% of sulfate aerosol particles contained soot impurities (this component is often called black carbon), whose sources may be products caused by airplane exhausts or biomass burning.

We can believe that internally mixed soot and sulfates make up a significant part of atmospheric aerosol on the global scale. This aerosol should be taken into account in estimating of both direct and indirect (through change of cloud properties) effect of aerosol on climate.

It follows from laboratory measurements that hygroscopic properties of soot depend on its composition. Organic substances on the surface of aerosol particles can increase adsorption of water, whereas such metals as Fe stimulate catalytic activity of soot. The data obtained in ASTEX/MAGE field experiment in the North Atlantic showed that soot is usually in the form of impurities in sulfate particles. Similar results were obtained over the oceans of the Southern Hemisphere in the ACE-1 experiment. The presence of soot particles functioning as heterogeneous nuclei possibly stimulates the formation of sulfate aerosol. Besides, soot particles covered with water film may serve efficient cloud condensation nuclei.

An important circumstance is that in the presence of aerosol particles as an internal mixture of sulfates and soot the direct aerosol-induced radiative forcing decreases markedly. The estimates showed that every percent of increase of the soot/sulfate mass ratio gives rise to positive RF at the atmospheric top level equal to 0.034 W/m<sup>2</sup>. This RF strongly depends, however, on the surface albedo, increasing as the albedo increases.

The effect of soot particles on the optical properties of clouds is rather complicated. On the one hand, particles generated due to biomass burning favor the increase of the cloud albedo due to a decrease in the size of cloud droplets. But, on the other hand, the presence of strongly absorbing soot-containing droplets intensify solar radiation absorption by clouds. To solve this problem, further investigations are needed.

The increasing rate of burning the fossil fuels and wood is the source of various optically active trace gases and aerosol particles in the atmosphere. An important component generated in the process of burning is total carbon (TC) including black carbon (BC) and organic carbon (OC) or particulate organic matter (POM), taking into account the effect of reactions with participation of oxygen and hydrogen (in this connection the following relation is accepted for mass transformation POM = 1.3 POM). The TC components are characterized by different optical and chemical properties. If the dominating bcq feature is its absorbing properties, then in the case of POM the main feature is scattering characteristics similar to those of typical of sulfates.

An importance of biomass and fossil fuel burning as a source of greenhouse gases motivated the interest to estimation of budgets of such burning products coming to the atmosphere as BC and POM. On the global scale and on the average over a year, the emissions of BC, POM, and aerosol due to burning of fossil fuels are comparable, and the main component of emissions is POM. Therefore, a particular attention should be paid to estimates of atmospheric emissions from forest fires in the middle and high latitudes.

In this connection, Lavoué et al.<sup>50</sup> obtained the estimates, which allowed compilation of the first maps of distribution of monthly particulate carbon emissions into the atmosphere due to forest, bush, and grass fires. In addition, statistical data on the areas of burnt territories, the mass of burnt organic matter, fire characteristics, and emission coefficients were given. Analysis of the data for the period of 1960\$1997 revealed the marked annual variability.

On the whole, the fraction of vegetation burning products makes up about 4% of the atmospheric emissions, but in some years it increases up to 12% with the contributions from BC and POM being equal to 9 and 20%, respectively. The absolute levels of the corresponding emissions due to fires in boreal forests of the North America (Canada and Alaska) vary within 4\$122 GgC/yr (BC) and 0.07\$2.4 Tg/yr (POM), whereas in Eurasia (Russia and Northern Mongolia) the variability ranges of 16\$474 GgC/yr (BC) and 0.3\$9.4 Tg/yr (POM) are possible.

As to the emissions due to forest fires in midlatitudes, these are, on the whole for the USA (continental part of the USA territory to the south from the Canada border) and Europe much lower and equal, on the average, to 11 GgC/yr (BC) and 0.2 Tg/yr (POM). The scales of grass fires in Mongolia are very large: 62 GgC/yr (BC) and 0.4 Tg/yr (POM). The mean annual emissions of BC due to bush fires

in Mongolia and California (totally) are 20 GgC/yr, and the POM emissions make up 0.1 Tg/yr. Table 1 gives the summary data on the emissions caused by vegetation burning. Reference 50 presents the maps of geographic distribution of emissions with 1° (latitude) × 1° (longitude) resolution.

#### 1.4. Sulfur cycle and sulfate aerosol

The particular importance of the sulfur cycle in the context of natural and anthropogenic climate changes defines the key role of sulfur compounds as atmospheric constituents. Although anthropogenic emissions of sulfur compounds in the Northern Hemisphere exceeded natural sources already many years ago, in the Southern Hemisphere the contribution of natural sources is still twice and even more as large as the contribution of anthropogenic emissions, and ocean is the most intense natural source of atmospheric dimethylsulfide. Under the Antarctic conditions, sulfur is a widespread element always present in atmospheric aerosol, making up to 80% 90% of the mass of aerosol deposited on Antarctic Plateau. Even in winter sulfur occupies the place just after Na and Cl, thus reflecting the effect of intense intrusions of marine air (salt storms) in such periods, when other sulfur sources are insignificant or absent at all.

Initially it was assumed that sulfur compounds come to Antarctica as a result of transport from the stratosphere or volcanic activity. However, further investigations showed that local volcanic sources can explain no more than 10% of sulfur budget. The sulfur inflow from the stratosphere is also of secondary importance, except for the cases of powerful volcanic eruptions. It turned out that the main natural source of sulfur for the Antarctic atmosphere is DMS emissions from the ocean. Correlation was found between blooming of *Phaeocystis* phytoplankton in the seas circumjacent Antarctica and many parameters connected with DMS. It became clear therefrom that the annual behavior of sulfur compounds in the Antarctic atmosphere reflects the sea biodynamics.

The above conclusions stimulated glaciologists to search for possible effect of sulfate aerosol on climate through analysis of cores of sea bottom sedimentary rock. The SCATE project was developed to study chemical processes determining DMS oxidation. Within the framework of this project, the concentrations of such trace gases as methanesulfonic acid in the gas phase MSA(g), dimethylsulfide, DMSO(g), SMSO<sub>2</sub>(g), and

H<sub>2</sub>SO<sub>4</sub>(g) were measured at the Palmer Antarctic station for the period from January 18 to February 25 of 1994 with the time step less than 15 min (Ref. 26).

Analysis of the obtained data suggested that the main source of DMSO is the reaction between DMS and OH, which is also responsible for production of MSA(g) at the successive oxidation of the products of DMSO and MSA. The OH/DMS reaction and the next reaction with the allowance for OH/DMSO are likely the main sources of SO<sub>2</sub>. No data evidencing that some intermediate compounds (for example, SO<sub>3</sub>), other than SO<sub>2</sub>, are the sources of H<sub>2</sub>SO<sub>4</sub> were found. Certainly, under conditions of the Palmer station, the considerable part of the DMS oxidation cycle occurs above the atmospheric boundary layer (ABL) in the so-called buffer layer.

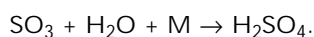
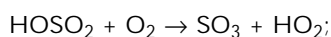
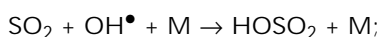
The main result obtained in observations and numerical simulation within the SCATE Project is close correlation found between the chemical processes and the atmospheric dynamics. The observations revealed frequent episodes of fast vertical transport from the very thin marine boundary layer to the upper-lying buffer layer. Due to the combination of the DMS long photochemical lifetime and frequent occurrence of intense convection in the ABL, a significant part of DMS emitted by the ocean comes to the buffer layer in the unoxidized state. In the buffer layer, which is characterized by the increased concentration of OH and weak aerosol scavenging, oxidized sulfur is accumulated up to high concentrations. Some portions of air from the buffer layer may sometimes come back to ABL, affecting the content of SO<sub>2</sub>, DMSO, and DMSO<sub>2</sub> in it. Besides, since SO<sub>2</sub> and DMSO are the main precursors of H<sub>2</sub>SO<sub>4</sub> and MSA, chemical processes in the buffer layer in combination with the vertical transport control the content of H<sub>2</sub>SO<sub>4</sub> and MSA in ABL.

In Ref. 26 it was emphasized that since the information about chemical processes in the Antarctic atmosphere is incomplete, the above conclusions are only tentative. This is caused, in the first turn, by the absence of data on the SO<sub>2</sub> content in the ABL, as well as the total lack of direct measurements of the concentration of both DMS and all oxidized sulfur compounds in the buffer layer. The details on the vertical transport between the ABL and the buffer layer and episodic air intrusions from the buffer layer to the ABL are unclear. It is also unclear whether the Palmer station is sufficiently representative.

Table 1. Emissions of carbon particles due to vegetation burning

Object of fire	Burnt biomass, Tg	Black carbon, TgC	Organic carbon, Tg
High- and middle-latitude forest	66\$700	0.07\$0.54	1.01\$10.70
Savannas, tropical forest, farm and house fires (according to Lioussé et al., 1966)	5375	5.63	44.50
Global biomass burning	5441\$6075	5.70\$6.17	45.51\$55.20
Contribution of middle- and high-latitude forests, %	1.2\$11.5	1.3\$8.8	2.2\$19.4

Aerosol sulfate is the main final form of sulfur compounds in the atmosphere that is produced in the process of sulfur oxidation. As a rule, reduced sulfur compounds in the process of their chemical transformations pass through the stage of oxidation (before transformation into sulfate) as  $\text{SO}_2$ . Oxidation of sulfur dioxide is the most important anthropogenic source of sulfate in the free troposphere, and the oxidation process proceeds in both the aqueous phase (heterogeneous process) and the gas phase (homogeneous reactions). Homogeneous oxidation is mostly determined by reactions with the participation of hydroxyl:



As to the process of heterogeneous oxidation, different variants of S(IV) transformation ( $\text{SO}_2$ ,  $\text{HSO}_3^\ominus$ , and  $\text{SO}_3^{2\ominus}$ ) into S(VI) are possible, and most efficient oxidants are  $\text{H}_2\text{O}_2$ ,  $\text{O}_3$ , and  $\text{O}_2$ . Savarino et al.<sup>74,75</sup> estimated the related significance of different heterogeneous oxidation reactions based on the analysis of isotopic composition ( $^{16}\text{O}$ ,  $^{17}\text{O}$ , and  $^{18}\text{O}$ ) of sulfates produced in these reactions. For this purpose, sulfur oxidation caused by  $\text{H}_2\text{O}_2$ ,  $\text{O}_3$ , and  $\text{O}_2$  and catalyzed by Fe(III) and Mn(II) was studied under laboratory conditions. In the case of oxidation in the gas phase, only the reaction  $\text{SO}_2 + \text{OH}$  mentioned above and its final phase  $\text{SO}_3 + \text{H}_2\text{O}$  were considered.

According to the results obtained, no one of the heterogeneous or homogeneous oxidation reactions can explain the observed mass-independent oxygen isotopic composition of sulfate. Since  $\text{H}_2\text{O}_2$  and  $\text{O}_3$  have the mass-independent isotopic signature, the possibility of transfer of this anomaly to sulfates was analyzed. The isotopic analysis showed that both of the oxygen atoms from  $\text{H}_2\text{O}_2$  are present in  $\text{H}_2\text{SO}_4$  as a final product of oxidation, but in the case of  $\text{O}_3$  only one oxygen atom comes into sulfate. Based on this, we can believe that the mass-independent oxygen isotopic composition of sulfate can be caused only by heterogeneous oxidation. This result allows, in particular, estimating the contributions of homogeneous reactions with the participation of OH and heterogeneous process with the participation of  $\text{H}_2\text{O}_2$  and  $\text{O}_3$  in sulfate production. The obtained results may prove useful also for checking the model adequacy to simulate chemical processes in the atmosphere with the allowance for transport.

Of particular importance is the problem of sulfate aerosol deposition onto forest, what can be illustrated by the results of some researches carried out in the USA<sup>22</sup> (see also Ref. 48). After adoption of the US Clean Air Act in 1970, emissions of sulfur dioxide decreased in most US states with only rare exceptions, including Georgia, where  $\text{SO}_2$  emissions almost doubled (increased by 88%) for the period of 1975–1985 and now occupy the seventh place in the USA. Since these emissions are an extreme

hazard for land and water ecosystems, a demand arose for the study of the processes of dry deposition and local wet scavenging of sulfur compounds (especially in forests) and the following estimation of the effect of deposited substances.

Sulfur dioxide emitted into the atmosphere can then deposit onto forests both in the gaseous form and in the form of sub-micrometer ( $(\text{NH}_4)_2\text{SO}_4$ ) or larger ( $\text{CaSO}_4$ ) aerosol particles produced in gas-phase reactions. Wet scavenging of sulfur, which largely defines the precipitation acidity, proceeds in the form of  $\text{SO}_4^{2\ominus}$  and can be estimated rather reliably, but in the case of dry deposition, this can hardly be made because of the complexity and variability of this process. However, it is significant that dry deposition of sulfur compounds on forest ecosystems (especially in the form of gaseous  $\text{SO}_2$ ) makes up a considerable part of deposition of acidifying components (very often more than 50%).

Since sulfur deposition is not a limiting factor for forest growth, until recently it did not attract such a great attention as in the case of other nutrients. However, increasing emissions of sulfur compounds into the atmosphere require intensification of such studies. In this connection, Cappellato et al.<sup>22</sup> studied the processes of dry deposition and wet scavenging of sulfur in coniferous and deciduous forests in the Panola Mountain watershed region (Georgia, USA).

According to the results obtained, the total (dry and wet) deposition for the period since October 1987 till November 1989 was 12.9 and 12.7 kg/ha · yr for deciduous and coniferous forests, respectively. The contribution of dry deposition (mostly due to  $\text{SO}_2$ ) achieved more than 40%. The sulfur inflow under the forest canopy (on the average for a year) turned out to be 37% higher in the deciduous forest than in the coniferous one. This can be explained by a considerable dry deposition. Although the sulfur inflow through deposition exceeds the trees growth needs, more than 95% of deposited sulfur was handled within the watershed mostly due to  $\text{SO}_2^{2\ominus}$  adsorption by iron oxides and hydroxyls contained in the soil. The content of sulfur in white oak and trunks of pine tree for the last 20 years increased by 200% (possibly, due to the increasing emissions).

The complexity of estimating the aerosol effect on climate dictates the need in obtaining more reliable information on the poorly studied aspects of this problem. One of such aspects is the hygroscopic growth of aerosol particles. Using a hygroscopic tandem differential mobility analyzer (H-TDMA), Berg et al.<sup>18a</sup> completed shipborne measurements of the hygroscopic properties of sub-micrometer aerosol in the marine boundary layer over the Pacific and Southern Oceans during ACE-1. The results of measurements show how the particle diameter changes in the process of evolution from the dry state to the relative humidity (RH) equal to 89–90%.

The initial values of the dry particle diameter were 35, 50, 75, and 150 (or 165) nm. The natural

background aerosol in MBL consists of two types with a significantly different hygroscopic behavior: sea-salt and non-sea-salt (NSS) components. Since the H-TDMA instrument could clearly distinguish between these two types of aerosol, it turned out to be possible to determine their contributions to the observed mixing aerosol.

During the ACE-1 intensive campaign in the Southern Ocean to the south of Australia, the hygroscopic diameter growth factors at RH = 90% for NSS aerosol particles were 1.62, 1.66, and 1.78 at dry particulate diameters of 35, 50, and 150 nm, respectively. These values far exceed the growth factors under conditions of polluted continental air mass. The growth factors for the externally mixed sea salt particles were even higher (2.12 and 2.14 for 50 and 150 nm). The corresponding values for the Pacific Ocean (at RH = 89%) for the NSS sulfate particles were 1.56, 1.59, 1.61, and 1.63 for 35, 50, 75, and 165 nm. The cases of particle solution and RH-hysteresis were observed only at RH = 68–90% in air masses to the north of the South Pacific circulation and only for Aitken mode particles (particle diameter within 20–80 nm). The occurrence of externally mixed sea salt particles could be linked to conditions with high wind speeds in connection with frontal passages or low pressure systems. However, it should be noted that the number density of externally mixed particles with the diameter of 150 nm weakly correlated with the local wind velocity (likely because of the long lifetime of these sub-micrometer particles). Particles having much lower growth factors than the NSS particles (they were called less hygroscopic particles) were observed only in the periods of anthropogenic effect.

Biomass burning is of particular importance in the context of the problem of aerosol effect on climate,<sup>14</sup> and this circumstance initiated the Biomass Burning Experiment (BIBEX). The main goal of this experiment was to evaluate the aerosol and gas emissions from biomass burning, as well as their effect on the chemistry of the global atmosphere and climate. The corresponding international field experiments were firstly conducted in the tropical belt of the Atlantic Ocean in the Southern Hemisphere (Amazon River basin, Atlantic tropics, South Africa), where the effect of fires in tropical forest and savanna is most pronounced. BIBEX projects included the TRACE-A (Transport and Chemistry near the Equator-Atlantic) American-Brazilian Program aimed at the study of biogenic emissions in Brasilia and their following transport and photochemical transformation. Based on co-operation between African, European, and American countries, investigations of atmospheric emissions from forest and savanna fires and gas emissions from burned soils were started. Initially, these investigations were called the SAFARI (Southern African Fire-Atmospheric Research Initiative) Program, but after agreement on co-ordination with the TRACE-A Project they were called STARE (Southern Tropical Atlantic Regional Experiment). These multidisciplinary field investigations started in the last part of 1992 and

were based on the use of various observation facilities (ground-based, shipborne, airborne, space-borne).

### 1.5. High-latitude atmospheric aerosol

Polissar et al.<sup>64,65</sup> analyzed the results of measurement of the chemical composition of aerosol based on the data of seven stations situated in Alaska (within the National Park) for the period of 1986–1995. The results of elemental analysis based on the concentration of soot (black) carbon and the total aerosol mass were obtained with the use of samples containing particles smaller than 2.5 μm in diameter. On the assumption that the source of all elemental sulfur is sulfate SO<sub>4</sub><sup>2s</sup>, the excessive (non-sea-salt) concentration of sulfates (XSO<sub>4</sub><sup>2s</sup>) was calculated through subtraction of the mass fraction of the sea-salt sulfates SO<sub>4</sub><sup>2s</sup>.

The mass concentration of XSO<sub>4</sub><sup>2s</sup> varied from 0.01 to 3.9 μg/m<sup>3</sup>, and the mass concentration of bc varied from 0.01 to 5 μg/m<sup>3</sup>. At almost all sites the annual behavior of the XSO<sub>4</sub><sup>2s</sup> concentration with a maximum in winter-spring and minimum in summer was observed. However, such an annual behavior was absent in the case of BC and fine aerosol. The amplitude of the annual behavior of XSO<sub>4</sub><sup>2s</sup> increased in northeastern Alaska. The maximum concentration of soot carbon in central Alaska was observed in summer due to BC emissions into the atmosphere from forest fires.

In the period under study, the decreasing Pb concentration trend was observed in central Alaska. The obtained results evidence of the presence of aerosol pollution due to long-distance transport, as well as regional and local sources, in the considered cases. The annual behavior of XSO<sub>4</sub><sup>2s</sup> could be connected with the long-range transport of sulfur compounds due to emissions in the mid-latitudes, as well as with the change in the rates of photochemical production of SO<sub>4</sub><sup>2s</sup> in fine aerosol and removal of fine aerosol from the atmosphere. Analysis of the spatial distribution of XSO<sub>4</sub><sup>2s</sup> revealed the presence of the pronounced negative gradient from the northwest to the southeast, which can be caused by the effect of the long-range transport of anthropogenic aerosol from sources situated to the north or northwest from Alaska.

The nature, origin, and transport of the arctic aerosol are the subjects of research for a long time. It was found, in particular, that considerable long-range transport of anthropogenic aerosol from different sources to Arctic occurs in winter and spring. In the period from 1986 to 1995 at seven sites of the Alaska's National Park, the composition of the fine (particles less than 2.5 μm) fraction of atmospheric aerosol was measured.<sup>64</sup> The obtained results were processed with the use of the new technique of factor analysis – the so-called positive matrix factorization (PMF). This technique provides for reliable consideration of such data that are absent or below the detection limit.

Analysis of the data by the PMF method revealed components caused by six sources. All the data point to the existence of soil component of aerosol in the presence

of a peak in the number density in summer and a minimum in winter. The sea-salt component was found at six points. In all (except for one) sites, black carbon,  $H^+$ , and K likely originating from forest fires were found. The universal components of aerosol are S, BC, Na, S, and Zn, Cu, and in three sites S, Pb and Br. Such components as S, Pb, and BC, Na, S are characterized by the annual trend with a maximum in winter-spring and a minimum in summer, and the amplitude of this trend increases with increasing latitude. The peculiarities of the annual behavior and the elemental composition of the components mentioned above are indicative of their anthropogenic origin from remote sources. The four main components of aerosol are anthropogenic aerosol coming through long-range transport (arctic haze), sea-salt aerosol, local aerosol of soil origin, and aerosol with high BC content generated by forest fires.

Kerminen et al.<sup>44</sup> analyzed the dependence of the physical-chemical properties of aerosol (changes in the chemical composition of aerosol depending on the particle size) obtained in the central part of the Greenland glacier in 1993–1995. The Aitken mode (particle diameter less than  $0.1 \mu\text{m}$ ), one or two modes of accumulation aerosol ( $0.1$ – $1 \mu\text{m}$ ), and super-micrometer particles were studied. Particles of the Aitken mode were characterized by relatively low total mass (less than 5%), but the highest number density. The accumulation mode is usually a superposition of two overlapping modes with the minimum particle diameter of about  $0.4 \mu\text{m}$ . The possible cause for this bimodality was particle processing by fog, which often occurred over the glacier in summer nights.

Sulfate, ammonium, methane, sulfonic acid, and dicarboxylic acid prevailed in the composition of particles of the accumulation mode, and these particles were likely the external mixture of sub-micrometer particles. The concentration ratio of MSA and sulfates varied depending on the particle size within the size range of the accumulation mode. Therefore, different ways of particulate deposition should lead to changes in the MSA/sulfates ratio.

Super-micrometer particles usually contained less than 20% of sulfates and more than 95% of nitrates. Sulfates and nitrates are likely the products of  $\text{SO}_2$  and  $\text{HNO}_3$  reactions with particles of rock origin. Super-micrometer sulfate particles have somewhat smaller size (less than  $3 \mu\text{m}$ ) than the nitrate ones ( $2$ – $3 \mu\text{m}$ ). Aerosol contains only a very small amount of semi-volatile acid compounds, except for the cases that plumes of biomass burning products penetrate into the glacier region. Such plumes are characterized by the increased level of low-volatile compounds, and they may contain sub-micrometer nitrate and ammonium formate particles.

In the period since June 1993 until June 1994 at the Greenland Summit ( $72^\circ 35' \text{N}$ ,  $37^\circ 38' \text{W}$ , 3220 m above the sea level), continuous measurements of the elemental composition of atmospheric aerosol (fractions of small and large particles) was conducted with the Proton-induced X-ray emission (PIXE) instrument.<sup>80</sup> In many aerosol samples, the concentration of Al, Si, S, Cl, K, Ca, Ti, Mn, Fe, Zn, Br, Sr, and Pb exceeded the

detection limit, and these elements originated from rocks, sea salts, and the anthropogenic sources (in the case of S and Br, some other sources are possible as well). The first of these sources was most pronounced in spring, while the anthropogenic source was equally significant during the whole year, but especially in winter and spring. It was usually difficult to find the presence of sea salt in the aerosol composition, but it was most marked in winter.

The results obtained in Ref. 80 were compared with the observations in the southern part of the Greenland ice sheet and at the North Station situated on the northeast coast of Greenland. At all these sites, the anthropogenic component peaked in winter and spring, when fuel burning was most intense, unlike Arctic, where the pronounced peak of the anthropogenic component is connected with the formation of arctic haze in early spring.

The data on chemical composition of deposited solid particles accumulated in the past by polar ice sheets are the source of information on the chemical composition of the pre-industrial atmosphere and its changes in different time scales. For example, analysis of ice cores yielded the data on the sea-salt and dust atmospheric aerosol, as well as the sulfate aerosol being the product of natural gas-phase reactions in the atmosphere. Interesting data were obtained for ammonium and light-weight carboxylic acids, what allowed reconstruction of the evolution of biogenic emissions.

Analysis of Greenland ice cores characterizing climate changes for the last 15 thousand years showed that in the last glacial period the background concentrations of ammonium and formic acid vapor were much lower than the current values. This was likely caused by decreased biogenic emissions into the atmosphere from soils and vegetations, because the large part of the North America was covered by ice. On the other hand, monitoring of the content of ammonium and formic acid in the atmosphere revealed considerable sporadic variations caused by biomass burning in high latitudes (forest fires), whose products reached Greenland.

In this connection, Savarino and Legrand<sup>74</sup> analyzed soluble admixtures in solid deposits accumulated in the ice core in central Greenland for the period of 1193–1767 (earlier these data were analyzed for the period of 1767–1980). Seventy three ice layers with the increased concentration of ammonium and formic acid due to the inflow of the products of biomass burning in the high latitudes were found. The chemical composition of the layers is characterized by the presence of the mixture of ammonium, formic acid, and nitrate with the polar ratio  $\text{NH}_4^+ / (\text{HCOO}^- + \text{NO}_3^-)$  close to unity. The differences in the chemical composition can be explained by different conditions of forest fires (relation between burning and smoldering) or meteorological conditions on the path of plume transport to Greenland.

Three periods of increased inflow of biomass burning products were separated out: 1200–1350, 1830–1930, and, to a lesser degree, 1500–1600. The period of 1200–1350 coincides with the phase of warm and dry climate

characteristic of medieval warming. After the low inflow of burning products in the Little Ice Age (1600–1850), it increased on the verge of the two last centuries, but decreased in the 20th century. Gradual decrease was noticed in the concentration of the formic acid, what can be explained by degradation of boreal forests in North America.

There are three sources of carbon aerosol in the atmosphere: natural primary and secondary emissions of organic gases by vegetations, fossil fuel burning, and biomass burning. The available data allow us to believe that the latter two sources (mostly anthropogenic) dominate in the global budget of carbon aerosol, and carbon aerosol is largely produced in the tropics (biomass burning) and mid-latitudes of the Northern Hemisphere (fossil fuel burning). Of particular interest is the production of carbon aerosol under urban conditions, while observations in remote regions characterize the background state.

Although the carbon aerosol is characterized by the presence of several forms with different chemical composition, their common property is the high carbon concentration. Usually two groups of carbon aerosol are distinguished: organic and soot (black) carbon. Though the latter usually makes up only a small part of the carbon aerosol, its measurements are most numerous because of their simplicity.

Measurements of the BC concentration with an aethalometer at the Halley Antarctic station in 1992–1995 were discussed in Ref. 8. Analysis of the results obtained revealed some episodes with the BC concentration increased due to local sources. However, such data were rather reliably removed from the consideration. Processing of the filtered data gave the pronounced annual behavior of the BC concentration with the mean monthly values varying from 0.3 to 2 ng/m<sup>3</sup> (these values somewhat exceed those observed at the South Pole). The peak in the annual behavior is observed in summer with the secondary (and common) maximum in October (the same behavior was observed at the South Pole, and it is similar to the annual behavior of the dust aerosol as judged from the data from the Neumayer coastal station). This annual behavior is likely determined by the process of biomass burning in the tropics subject to strong modulation due to the processes of BC transport in the Antarctic region (the corresponding mechanisms were not reliably reconstructed by numerical simulation).

The BC concentration turned out to be too low to affect the snow cover albedo in Antarctica. Similarity of observations at the Halley station and the South Pole indicates that analysis of data on BC in ice cores reliably represents the BC paleoevolution in Antarctica and, in particular, serves as an indicator of biomass burning in the Southern Hemisphere.

### 1.6. Dust aerosol from deserts

This issue has received sufficient consideration in the scientific literature.<sup>2</sup> The Sahara Desert is one of

the powerful sources of dust atmospheric aerosol. To continue the earlier investigations of the consequences of the Saharan dust aerosol transport across the Atlantic Ocean, Li-Jones and Prospero<sup>51</sup> discussed the results of every-day filter and impactor measurements of the aerosol concentration and microstructure at Barbados (13°15' N, 59°30' W) in the period since April 5 until May 3 of 1994, during which four episodes of Saharan dust transport reaching Barbados were observed.

Processing of the observations has enabled revealing high correlation between the concentrations of the non-sea-salt sulfate aerosol (NSS SO<sub>4</sub><sup>2s</sup>) and dust ( $r^2 = 0.93$ ). The mass concentrations of aerosol varied, respectively, from 0.5 to 4.2 and from 0.9 to 257 μg/m<sup>3</sup>. Diurnal variations of the aerosol microstructure proved to be insignificant for both types. However, the coarse particle fraction (CPF) (particles with the aerodynamic diameter larger than 1 μm) of the non-sea-salt sulfate aerosol varied markedly (from 21 to 73%).

The maximum values of CPF SO<sub>4</sub><sup>2s</sup> were connected with the influx of the Saharan dust (as evidenced by the data of satellite observations), and the minimum values corresponded to the invasion of air masses from the North Atlantic, where the dust concentration was lower than 0.9 μg/m<sup>3</sup>. It was assumed in Ref. 51 that high values of CPF SO<sub>4</sub><sup>2s</sup> follow from heterogeneous reactions between SO<sub>2</sub> contained in the polluted air from Eastern Europe and the Saharan dust in the atmosphere over North Africa.

However, the interaction between pollutants and dust not always manifests itself in the high CPF. The low CPF is indicative of the process of SO<sub>2</sub> oxidation to SO<sub>4</sub><sup>2s</sup> occurring before the dusted air comes. On such days, the dominant source of NSS SO<sub>4</sub><sup>2s</sup> is likely oceanic dimethylsulfide, and under these conditions CPF remains close to 20%. Since the episodes of the Saharan dust emission give rise to marked changes in the microstructure of NSS SO<sub>4</sub><sup>2s</sup>, the effect of the mineral dust on the NSS SO<sub>4</sub><sup>2s</sup> microstructure should be taken into account when estimating the effect of the non-sea-salt aerosol on the radiative transfer in the atmosphere.

The dust-induced removal of the most radiatively efficient fraction of the sulfate aerosol from the atmosphere should lead to a significant decrease of the radiative forcing due to the sulfate aerosol. Naturally, this is most pronounced in the regions, where the episodes of dust emissions are most frequent (in significant part of Asia and Indian sub-continent). Of great importance is also the dust-induced removal of SO<sub>2</sub> from the atmosphere, which can manifest itself in the regions far from the sources of dust emissions, as, for example, at Saharan dust transport across the Atlantic Ocean or Mediterranean Sea (in the direction toward Western Europe).

### 1.7. Aerosol models

The adequate allowance for the effect of atmospheric aerosol on climate calls for consideration of the whole

variety of its types and the wide space-time variability of aerosol properties due to numerous sources and short aerosol lifetime.<sup>39,47,48</sup> It is just for these reasons the results of local measurements of aerosol properties cannot be considered as representative for large space-time scales. The only reliable method of solving the problem is, on the one hand, to use data of direct (ground-based, airborne, balloon-borne) measurements of aerosol properties and satellite remote sensing and, on the other hand, the results of numerical simulation (verified by observations) of aerosol transport in the atmosphere (with the allowance for its transformation and production from the gas phase through gas-phase reactions). Numerical simulation should provide for reconstruction of the realistic space-time variability of aerosol properties on the global scale. Only in this way we can obtain adequate information about the global fields of aerosol properties needed for calculation of the aerosol-induced radiative forcing and following estimation of the aerosol effect on climate.

In this connection, Tegen et al.<sup>77,78</sup> simulated numerically the global aerosol distribution for four types of aerosol (soil dust, sulfate, sea-salt, and carbon) using the global model of aerosol transport in the atmosphere. In description of the dust aerosol transport, the dependence of the dust inflow to the atmosphere on the humidity and soil texture, wind velocity near the surface, and surface conditions was taken into account. The source emission rate and dust aerosol transport were calculated for eight classes of particle size in the range from 0.01 to 10  $\mu\text{m}$ . The information about the wind velocity was obtained from the data of the European Centre for Medium-Range Weather Forecasts on a  $1.125^\circ \times 1.135^\circ$  grid with the time step of 6 h (this allows the data on dust aerosol emissions to be updated every six hours). The three-dimensional global model of transport of passive admixtures developed in the Goddard Institute for Space Studies (GISS) has nine levels on a  $4^\circ \times 5^\circ$  grid. The dust aerosol is removed from the atmosphere through dry deposition and wet scavenging. The atmospheric lifetime of the dust aerosol varies from 230 h for 0.15- $\mu\text{m}$  particles (they are mostly removed by precipitation) to 30 h for 8- $\mu\text{m}$  particles (gravitational sedimentation).

The model provides for calculation of global fields of not only the number density, but also of the aerosol microstructure. The transport of the marine sea-salt aerosol (MSA) was calculated in a similar way, but in this case the aerosol concentration in the atmosphere was calculated, rather than its emissions (as in the case of dust aerosol). The microstructure is characterized by six size intervals within 2–16  $\mu\text{m}$ . The main processes of  $\text{I S}^-$  removal from the atmosphere are its dry deposition and wet scavenging. About 70% of  $\text{I S}^-$  mass is concentrated in the lower 5-km tropospheric layer.

The comparison of the results of numerical simulation of the MSA annual behavior with observations showed rather close agreement. Since the sea surface is

continuously active as an MSA source (except for the polar regions), it is natural that MSA is characterized by not that wide space-time variability as the dust aerosol. For the sulfate aerosol, the global model developed in the GISS allows the field of the sulfate aerosol to be reconstructed with the allowance for the sources, sinks, and gas-phase transformations of  $\text{SO}_2$ , dimethylsulfide, methanolsulfide, and  $\text{SO}_4^{2-}$ .

The available estimates show that fossil fuel burning (on the global scale) is responsible for 68% of emissions of sulfur compounds, and the contribution of  $\text{SO}_4^{2-}$  is 49 MtS. The calculations showed that the lifetime of sulfur aerosol in the atmosphere is 3.9 days. The comparison of the estimated emissions and the concentration of sulfates revealed both some similarity and significant difference. The global field of carbon aerosol including both organic and soot aerosol was simulated with the GRANTOUR 12-level model on the  $4.5^\circ \times 7.5^\circ$  grid, in which the wind and precipitation fields are specified based on the data for the CCM-1 climate model developed in the US National Center for Atmospheric Research. Emissions from burning of biomass (fire-wood burning, charcoal burning and production, forest and savanna fires, etc.) and fossil fuel were estimated, as well as natural sources of organic carbon.

The calculations of the global sources of carbon aerosol gave the following estimates: biomass burning \$ 45 Mt/yr (including 6 Mt/yr of soot carbon) and fossil fuel burning \$ 29 Mt/yr (including 7 Mt/yr of soot carbon). The contribution of natural sources is about 8 Mt/yr of organic matter. Model emissions of aerosol due to biomass (fossil fuel) burning were considered in the lower 2-km (1-km) atmospheric layer. The calculated results as a whole are in agreement with observations, but they depend very strongly on the scavenging factor and the height of the emission level. To calculate the aerosol optical depth (AOD)  $\tau$ , one should know the aerosol content (mass) in the atmospheric depth  $m$ , the effective particle radius  $r_{\text{eff}}$  (or aerosol microstructure), and the particle refractive index. If  $Q_{\text{ext}}$  is the wavelength-dependent dimensionless extinction coefficient, then approximately  $\tau = 3 Q_{\text{ext}} m / 4 \rho r_{\text{eff}}$ , where  $\rho$  is the particle density, or  $\tau = B m$ , where  $B = 3 Q_{\text{ext}} / 4 \rho r_{\text{eff}}$  is the so-called specific extinction cross section.

The information about the vertical aerosol distribution (especially, concerning the absorbing aerosol) is of particular importance (in the context of the aerosol effect on climate). Table 2 gives the values of the emission rates of aerosol sources and the calculated optical characteristics for different types of aerosol.

In this case, the aerosol was not differentiated into natural and anthropogenic. As is seen from Table 2, the contribution of the soil dust aerosol to the mean global AOD is comparable with the contributions of sulfates and carbon aerosol (about 85% of sulfate aerosol is produced due to oxidation in clouds in the regions with most

intense precipitations, what defines the dominant role of wet scavenging as an aerosol sink).

**Table 2. Mean global values of emission rate and total content and optical characteristics of different types of aerosol**

Type of aerosol	Source emission rate, Tg/yr	Mean content, mg/m <sup>2</sup>	$B$ , m <sup>2</sup> /g	Optical depth (mean)	Optical depth (maximum)
Sea-salt aerosol	5900	22.4	0.2\$0.4 (0.3) <sup>a)</sup>	0.007	0.02
Soil dust (1\$10 μm)	1000	21.6	0.2\$0.4 (0.3)	0.007	0.59
Soil dust (< 1 μm)	250	14.7	1\$2 (1.5)	0.022	0.85
Sulfate aerosol (H <sub>2</sub> SO <sub>4</sub> ) <sup>b)</sup>	150	3.0	5\$12 (8.0) <sup>c)</sup>	0.025	0.26
Carbon aerosol <sup>d)</sup>	81	2.5	5\$12 (8.0)	0.019	0.25
Soot aerosol	12	0.3	8\$12 (9.0)	0.003	0.05

Notes: <sup>a)</sup> the value in parenthesis is that taken for AOD calculation (all the data correspond to the wavelength of 0.55 μm);

<sup>b)</sup> it is assumed that the sulfate aerosol consists of H<sub>2</sub>SO<sub>4</sub>;

<sup>c)</sup> the values obtained over land and ocean are equal to, respectively, 5\$8.6 (6.0) and 7\$14 (10) m<sup>2</sup>/g;

<sup>d)</sup> carbon aerosol includes the soot component.

Application of the calculation technique described above allowed the global maps of the AOD distribution in different seasons to be drawn. These maps reconstruct reliably such regularities as, for example, the annual behavior of the Sahel maximum of AOD (which is determined here by the contributions of dust and carbon aerosol); the peaks of aerosol content in the regions of China (in spring) and Saudi Arabia (in summer) due to dust aerosol. Dust aerosol carry-over from North Africa to the North Atlantic turned out to be underestimated (because of systematic underestimation of the calculated maximum wind velocity). In the Southern Hemisphere, AOD has increased values over the Pacific Ocean around Australia, what is likely connected with dust aerosol carry-over. The plume of biomass-burning aerosol is clearly seen over the Atlantic Ocean to the east from South America.

Comparison of the calculated global AOD fields with observations at a solar photometer network (these observations are of particular interest, since AOD is reconstructed from the satellite data only over the ocean) confirmed, on the whole, that the results of numerical simulation are quite realistic, but numerous significant differences were revealed as well (it is clear that different scales of space-time averaging and other circumstances seriously complicate this comparison). Comparison with the data of satellite observations over the ocean at clear sky can be considered more correct, though in this case the imperfection of the algorithms of AOD reconstruction introduces some restrictions. The results of AOD reconstruction from the NOAA/AVHRR data were used for this purpose. However, the use of these results allows only qualitative evaluation of the agreement between the calculated and observed AOD fields because of imperfection of the results of both the observations and numerical simulation.

The calculated data reliably reconstruct the annual AOD behavior, but, on the other hand, significant quantitative differences can be found. The results considered above indicate that any approximation of the global aerosol by some single model or even a set of

statistical models (urban, rural, background aerosol, etc.) fixed in space and time is unacceptable for numerical simulation of the aerosol effect on climate. The global fields of aerosol properties should be considered separately as applied to the main types of aerosol, keeping in mind that the following integration of models will account for variation of the aerosol composition. The realistic global aerosol climatology needed for numerical simulation of climate can be justified only through joint analysis of ground-based and satellite observations, as well as the results of numerical simulation.

Unfortunately, the complex system of global observations of aerosol properties is not yet organized (therefore all available observations are fragmentary), and even not justified. The hyperbolic attention paid recently to purely scattering aerosol causes particular concern, because the actual aerosol (taking into account its complex composition) is always absorbing, what certainly complicates its consideration in the theory of climate. According to the mean global estimates, the contribution of absorbing aerosol to AOD varies within 24\$53% (9\$46% over the ocean and 17\$34% in the industrial regions of the USA and Europe). Under the conditions of Western Europe, the contribution of only soot aerosol may achieve 20%. It follows from observations that the organic component of aerosol makes up about a half of the total aerosol mass near the northeastern coast of the USA. But according to the model data (see Table 2), the contribution of this component is roughly equal to the half contribution of the sulfate aerosol. In the regions of China and Sahel the contribution of the absorbing aerosol achieves 37\$71%. The wide space-time variability of aerosol properties causes the need in the development of an interactive aerosol block for climate models responsible for reconstruction of the actual dynamics of atmospheric aerosol properties.

Refined estimates of the emission rates of the global sources (precursor gases) of aerosol and aerosol emissions into the atmosphere can be found in Chapter 5

of IPCC Report-2001 (Ref. 39) and they are partly presented in Tables 3 and 4.

**Table 3. Emission rate of current sources of minor gases (MG) & aerosol precursors (Tg N, S, or q a year). Northern Hemisphere (NH) and Southern Hemisphere (SH)**

MG	NH	SH	Globe	Possible range
<b>NO<sub>x</sub>, TgN/yr:</b>				
Fuel burning	19.9	1.1	21.0	\$
Aviation	0.43	0.03	0.46	\$
Biomass burning	3.3	3.1	6.4	\$
Soil	3.5	2.0	5.5	\$
Farm soil	\$	\$	2.2	0\$4
Natural soil	\$	\$	3.2	3\$8
Lightning strokes	3.7	2.4	7.0	2\$12
<b>NH<sub>3</sub>, TgN/yr:</b>				
Domestic animals	17.5	4.1	21.6	\$
Farming	11.5	1.1	12.6	\$
People	2.34	0.31	2.6	\$
Biomass burning	2.5	2.2	5.7	\$
Fossil fuel burning and industry	0.29	0.01	0.3	\$
Natural soil	1.36	1.07	2.4	\$
Wild animals	0.10	0.02	0.1	\$
World Ocean	3.65	4.50	8.2	\$
<b>SO<sub>2</sub>, TgS/yr:</b>				
Fossil fuel burning and industry	68	8	76	\$
Aviation (1992)	0.04	0.003	0.04	\$
Biomass burning	1.2	1.0	2.2	\$
Volcanoes	6.3	3.0	9.3	\$
<b>DMS or H<sub>2</sub>S, TgS/yr:</b>				
World Ocean	11	13	24	\$
Land and soil biota	0.6	0.4	1.0	0.4\$5.6
<b>Volatile and organic compounds, Tgq/yr:</b>				
Anthropogenic	\$	\$	109	\$
Terpenes	67	60	127	\$

**Table 4. Primary emissions of aerosol particles into the atmosphere according to the data of 2000, in Tg/yr; *d* is particle diameter**

Type of aerosol	NH	SH	Globe		
			Mean	Minimum	Maximum
<i>Organic matter</i> (0\$2 μm)					
Biomass burning	28.0	26.0	54.3	45	80
Fossil fuel	28.4	0.4	28.8	10	30
<i>Black carbon</i> (0\$2 μm)					
Biomass burning	2.9	2.7	5.6	5	9
Fossil fuel	6.5	0.1	6.6	6	8
Aviation	0.005	0.0004	0.006	\$	\$
Industrial dust etc.			100	\$	\$
<i>Biogenic aerosol</i> (0\$2 μm)					
<i>Sea salts</i>			50	10	100
<i>d</i> < 1 μm	23	31	54	18	100
<i>d</i> = 1\$16 μm	1420	1870	3290	1000	6000
Total	1440	1900	3340	1000	6000
<i>Mineral (soil) dust</i>					
<i>d</i> < 1 μm	90	17	110	\$	\$
<i>d</i> = 1\$2 μm	240	50	290	\$	\$
<i>d</i> = 2\$20 μm	1470	282	1750	\$	\$
Total	1800	349	2150	1000	3000

## 2. Long-range transport and vertical diffusion

The atmosphere plays a major role in transport of various substances of natural and anthropogenic origin

from land to the World Ocean. In particular, aerosol particles from < 0.1 to > 10 μm in diameter can be transported to the distance as long as 10 000 km. The amount of transported substance turns out to be rather large. On the global scale, atmospheric transport of various trace elements to the ocean may exceed

their income due to river run-off. Since the atmospheric aerosol usually holds trace element content during transportation, its chemical composition and microstructure carry the important information about its sources and ways of long-range transport. In particular, the corresponding natural and anthropogenic contributions can be calculated. Let us illustrate some results obtained in this connection.

To recognize the sources and reveal the ways of aerosol transport during the Aerosol Oceanic Chemistry Experiment (AEROCE), Huang et al.<sup>37</sup> studied the time dependence of the trace element content in aerosol samples taken at the Bermudas in the period from 1988 to 1994. The elements originating from the earth's core (for example, Al) or from the sea (for example, Na) are characterized by the annual behavior with the maxima in summer and winter, respectively. On the contrary, the elements connected with anthropogenic sources of pollution (for example, Sb), are characterized by the presence of unusual semiannual behavior with pronounced maxima in spring and smaller fall maxima, which was not found earlier. The annual behavior of the trace elements is largely determined by the peculiarities of their long-range transport. Thus, for example, the spring maximum of aerosol pollution is caused by the fast east-west transport from the region of North America, and the fall maximum is caused by slow transport of the North-American air toward the Bermudas under the effect of quasistationary anticyclones over the Atlantic Ocean.

The low concentration of aerosol pollutants in winter is the consequence of southwestern spread of high-pressure systems from the Bermudas-Azores region. These systems provide for income of humid air to the Bermudas from the east or from the north-east and prevent the transport from North America and Africa. The summer maximum of pollutants is connected with air mass transport from East Atlantic and Africa. The variations of O<sub>3</sub> and CO, as well as two radionuclides of natural origin (<sup>210</sup>Pb and <sup>7</sup>Be) are characterized by the semiannual behavior similar to a cycle.

The aerosol composition in the Mediterranean atmosphere is largely determined by three sources: (1) anthropogenic sources located at the north and north-east; (2) soil aerosol carry-over from North Africa, especially, at dust storms (15-20 episodes every year); (3) inflow of marine aerosol over the Mediterranean Sea. In this connection, Güllü et al.<sup>33</sup> discussed the results of analysis of the elemental and ion composition of more than 600 aerosol samples collected for the period from March 1992 to December 1993 at the Turkish coast of the Mediterranean Sea 20 km to the west from Antalya (36.47°N, 30.34°E).

The concentration of elements of the soil origin turned out to be lower than in the western region of the Mediterranean Sea, what is caused by the longer range of transport of soil aerosol particles from Sahara. The concentration varied with time in the scale from days to seasons. Short-term variations in the aerosol concentration due to industrial pollution were connected

with the varying conditions of aerosol transport from its sources, and in the case of the sea-salt and soil aerosol the major role was played by the episodic character of its wind-driven inflow to the atmosphere.

The attempts to explain the long-term variations of the aerosol composition by the dynamics of long-range transport failed because of the absence of data on the annual variations of the long-range transport. The annual behavior of the concentration of anthropogenic elements is determined, first of all, by the variability of the process of wet scavenging. As to long-term variations in the composition of the marine and soil aerosol, they are largely determined by variations in the emission rates of the aerosol sources.

For one year Pirjola et al.<sup>63</sup> measured the aerosol microstructure at the Varrjo Research Station (67°46' N, 29°35' E) located at the height of 400 m above the sea level near the Russian border. The atmosphere in this region is usually very clean, but sometimes it is polluted due to emissions from metallurgic plants in Monchegorsk and Nikel separated from the station by less than 200 km. Observations of two episodes of inflow of industrial air and one episode of air transport from the south were discussed along with the results of numerical simulation of the change in aerosol properties with the allowance for the long-range transport and chemical processes.

One of the purposes of numerical simulation was to analyze the validity of the assumption, according to which the observed concentration of particles of nucleation mode can be explained by the effect of only homogeneous nucleation of sulfuric acid and water vapor (H<sub>2</sub>SO<sub>4</sub>/H<sub>2</sub>O). In the three episodes of polluted air inflow, the calculated particle number density turned out to exceed the observations by about an order of magnitude. Therefore, we can assume that particles under actual conditions were produced due to H<sub>2</sub>SO<sub>4</sub>/H<sub>2</sub>O nucleation.

Overestimation of model values may be caused by either overestimation of the nucleation rate (within the framework of the classic theory) or because of the assumption of clouds absence. In the case of air mass transport from the south, the calculated concentration turned out to be lower than observations, but in this case the possibility of H<sub>2</sub>SO<sub>4</sub>/H<sub>2</sub>O nucleation also cannot be excluded. For the two marine air masses, the calculated concentration of nucleation mode particles was close to zero, and therefore these particles were obviously produced due to some mechanism different than that for industrial particles.

One of the consequences of the fast economic development of South Korea and China in two recent decades is a considerable deterioration of the air quality, and long-range (transborder) transport of such pollutants as yellow sand, SO<sub>2</sub>, and sulfates contributes especially markedly to this deterioration. That is why Park and Cho<sup>61</sup> calculated the transborder transport, transformation, and deposition (dry and wet) of pollutants using the Sulfur Transport and Emissions Model (STEM II). STEM II was run for 72 h starting from 9 a.m. LT of

November 25 of 1989 with light precipitation for the last 36 hours.

The analysis of the results of numerical simulation showed that the calculated NO and SO<sub>2</sub> concentrations agree well with the observations, but the calculated O<sub>3</sub> concentration turned out to be underestimated because of unreliable input data on volatile organic compounds (VOC). Fast scavenging of such water-soluble components as H<sub>2</sub>O<sub>2</sub> and HNO<sub>3</sub> had a particular importance. The most intense wet scavenging was observed in the regions of intense precipitation.

For sulfates, the motion of the centers of their high concentration was clearly seen, but it was not the case with SO<sub>2</sub>. In Ref. 61, the air pollution transport index was justified that characterizes the effect of long-range transport on the air quality. It was shown that under some meteorological conditions the long-range transport of SO<sub>2</sub> and sulfates from Eastern China prevails over local emissions.

Using the one-dimensional Lagrangian model including a block describing chemical reactions of production of sulfur compounds and heterogeneous effects of interaction with sulfate aerosol particles and cloud droplets, Mari et al.<sup>52</sup> calculated the vertical concentration profiles for six components: (1) DMS emitted by the ocean, (2) SO<sub>2</sub> produced at DMS oxidation, (3) non-sulfate secondary sub-micrometer (NSS) aerosol in dry air produced at oxidation of SO<sub>2</sub> with participation of OH or through oxidation of SO<sub>2</sub> in sea-salt aerosol particles; (4) secondary NSS sulfates in cloud water (SO<sub>4</sub><sup>2-</sup>C) produced at heterogeneous oxidation of SO<sub>2</sub> in cloud droplets or through assimilation of NSS sulfates of dry air at cloud formation; (5) sub-micrometer aerosol of methanesulfonate (MS) in dry air produced at oxidation of DMS; (6) methanesulfonate in cloud water (MSS) produced by assimilation of MS of dry air during condensation of cloud droplets.

The considered model allows pre-calculation of the entrainment rate, characteristic values of the mixing height, and the frequency of cloud occurrence at the given field of geostrophic wind and large-scale deposition based on the data of objective analysis made in the European Centre for Medium-Range Weather Forecasts, and the ocean surface temperature field based on the data of shipborne observations. The model accounts for the processes of gas-phase and heterogeneous oxidation of SO<sub>2</sub> to NSS sulfates in clouds and the presence of the sea-salt aerosol.

Comparison of the results of numerical simulation with the observations of evolution of the model dynamic variables in the atmospheric depth demonstrated close agreement. The model adequately describes 82% of the observed variability of the DMS concentration on the assumption that the only oxidant is OH. However, uncertainties in the DMS oxidation rate and shipborne observations of the regional variability of the DMS concentration in sea water are too large for reliable determination of the rate of DMS transport from the ocean to the atmosphere. The calculated SO<sub>2</sub> mixture

ratios agree with observations at the efficiency of DMS transformation into SO<sub>2</sub> taken to be about 70%.

The calculations revealed the dominant role of SO<sub>2</sub> oxidation in sea-salt aerosol particles as a process controlling the SO<sub>2</sub> lifetime at least within the well mixed lower atmospheric layer. The neglect of heterogeneous loss of SO<sub>2</sub> markedly decreases the reliability of numerical simulation. In the presence of clouds, cloud droplets and the sea-salt aerosol contribute roughly equally to the heterogeneous losses. The calculated content of methanesulfonate in aerosol particles agrees well with the observed values. Some systematic errors arise in calculation of the concentration of NSS sulfates revealing only about one third of the observed variability. In the absence of clouds and at a gentle breeze, NSS sulfates are produced in photochemical processes, but in the presence of clouds the major role is played by oxidation in cloud droplets and in the sea-salt aerosol particles.

Numerical simulation of the global aerosol field with the allowance for the long-range transport and chemical reactions has received wide development in recent years, especially, as applied to sulfate aerosol. The role of sulfate aerosol in formation of clouds, acid precipitation, and climate is now commonly recognized. According to the current estimates, about 67 Tg of anthropogenic sulfur (98% in the form of SO<sub>2</sub>) and 15–23 Tg of sulfur having the biogenic origin are emitted annually into the atmosphere. The earlier estimates stated that the relative contribution of anthropogenic sulfur to the global sulfur budget makes up 35–75%. Using the CCM-3 global climate model developed in the US National Center for Atmospheric Research, Barth and Church<sup>15</sup> calculated the space-time variability of sulfate fields in two regions with the strongly polluted atmosphere: Mexico City and southeastern China.

Although the level of sulfate emissions in Mexico City (19°N, 99°E, 2.2 km above the sea level) is not extraordinarily high (as compared with other large industrial centers), the following two circumstances are of great importance: (1) specificity of meteorological conditions in this subtropical region (gentle breeze, characteristic combination of the dry and wet seasons); (2) the need in accounting for the components similar to the organic and carbon (black) aerosol and tropospheric ozone. It is a significant feature of the southeastern China the presence of not only anthropogenic emissions of sulfates, but also the carbon aerosol and such trace components as NO<sub>x</sub> and tropospheric ozone under the conditions of domination of the winter and summer monsoons accompanied by intense precipitation and, consequently, scavenging of sulfate aerosol from the atmosphere.

The CCM-3 interactive spectral T42 (2.8° latitude × 2.8° longitude) 18-level chemical-climatic model contains a block describing the kinetics of reactions, which determine the sulfate aerosol concentration field with the allowance for both anthropogenic and biogenic sources. The model covering the atmospheric depth up

to the pressure level of 5 hPa was realized with the time step equal to 20 min.

The analysis of the results of numerical simulation showed that sulfates emitted into the atmosphere in the region of Mexico City are mostly transported to the west and north, and from southeastern China they are transported to the east (moving around the globe in summer and fall). The contribution of Mexico City to the global anthropogenic sulfate emissions is about 1% with the fraction in the global sulfate budget also roughly equal to 1%. For southeastern China, the corresponding values are 11.6 and 9% with the nonlinear relationship between the emissions and budget of sulfates. If sulfate emissions in Mexico City are doubled, then their fraction in the budget doubles too, while under the conditions of southeastern China it increases more than twice. Under these conditions, the gas-phase mechanism of sulfate aerosol production plays a significant role and, thus, aerosol is less subjected to wet scavenging.

The qualitative estimates suggested that hydrophilic carbon aerosol has roughly the same lifetime as the sulfate aerosol in both regions under consideration. If hydrophobic carbon aerosol is emitted into the atmosphere and its transformation into the hydrophilic form takes about 1.9 days (what is roughly equal to the lifetime of sulfate aerosol), then the lifetime of the hydrophilic carbon aerosol turns out to be 3.5 days longer than that of the sulfate aerosol. In the case that transformation takes 5 days, the hydrophilic carbon aerosol can be found in regions with light cloudiness, where its lifetime increases up to 10 days and more.

Restad et al.<sup>69</sup> simulated numerically the three-dimensional global field of the tropospheric concentration of dimethylsulfide, sulfur dioxide, and sulfates using the OSLO CTM-1 model, which describes not only transport, but also chemical transformation of the considered components. The accounted-for combination of chemical reactions that allow describing the space-time variability of these components provides for approximate parameterization of heterogeneous oxidation and agrees rather well with observations, especially, under conditions of a polluted atmosphere.

The analysis of the obtained results showed that the essential amount of sulfates is transported in winter to Arctic (as evidenced by the observations as well). According to the calculations, the high level of the sulfate concentration is characteristic of the upper troposphere to the north from 20°N (especially in summer), what is caused by the low intensity of sinks. Some discrepancies take place between the calculated data and observations under conditions of marine background atmosphere (systematic overestimation of the SO<sub>2</sub> concentration, but underestimation of the SO<sub>4</sub><sup>2s</sup> concentration in tropics in summer in high latitudes). These discrepancies may be connected with the approximate consideration of the processes of heterogeneous oxidation, although the effect of inadequate reconstruction of the oxidation trajectory  $\text{DMS} \rightarrow \text{SO}_2 \rightarrow \text{SO}_4^{2s}$  also cannot be excluded. The considered results point to the need in further observation of emissions, as well as further

study of the processes of chemical transformation of natural sulfur compounds into SO<sub>2</sub> and sulfates.

The considerable attention paid now to the study of the effect of atmospheric aerosol on chemical processes in the atmosphere and climate is connected, in particular, with analysis of the role of hydrophilic aerosol as cloud condensation nuclei. It is important that about 20–50% of fine continental aerosol in mid-latitudes consist of organic compounds, and in tropic regions covered by forests this fraction can achieve 90%. The significant part of the organic component of aerosol consists of water-soluble and, probably, multifunctional compounds.

According to the available estimates, from 30 to 270 Tg/yr of organic aerosol on the global scale can be produced due to oxidation of biogenic compounds; this value is comparable with the scales of production of the biogenic and anthropogenic sulfate aerosol.<sup>41</sup> However, the possible evolution of the source of secondary organic aerosol functioning since the onset of the industrial epoch is yet poorly studied. Nevertheless, the anthropogenic effect on production of the secondary organic aerosol calls for serious consideration, because of the current increase in the concentration of oxidants (ozone, nitrate, hydroxyl radicals). Just the secondary organic aerosol can be the main component of condensation nuclei and cloud condensation nuclei over continents in the post-industrial epoch.

Kanakidou et al.<sup>41</sup> estimated the contribution of the secondary organic aerosol produced in ozonolysis of biogenic volatile organic compounds to the global field of organic aerosol and the evolution of the secondary organic aerosol after the onset of the industrial epoch using the MOGUNTIA three-dimensional global model of the troposphere, which accounts for both the transport processes and chemical reactions, in particular, oxidation of carbon monoxide, methane, and non-methane hydrocarbons C<sub>2</sub>–C<sub>5</sub> (NMHC), including isoprene. MOGUNTIA was run for one year (with the initial one-month period in the speed-up mode). Biogenic volatile organic compounds were characterized as a mixture of  $\alpha$ - and  $\beta$ -pinenes using the laboratory measurements of the rates of the corresponding reactions (including the gas-phase production of aerosol). An important factor in production of the secondary organic aerosol is deposition of the condensed oxidation products onto organic aerosol particulates existing earlier (this factor was taken into account in the model).

The emission rate of the global source of the secondary organic aerosol was estimated as 17–28 Tg/yr in the pre-industrial epoch and 61–79 Tg/yr nowadays. This three- to four-fold intensification of the organic aerosol production from biogenic volatile organic compounds can be explained by the anthropogenically caused growth of the ozone and organic aerosol content in the troposphere. The most important sources of errors in the obtained results are the uncertainty in the data on the composition of biogenic volatile organic compounds and approximate parameterization of gas-phase aerosol production processes. The inevitable future industrial development of the countries situated in the

tropical and subtropical zones will lead to the increase in atmospheric emissions of nitrogen oxides NO<sub>x</sub> and organic matter produced at biomass and fossil fuel burning, and this, in its turn, will certainly affect the concentration of the organic aerosol in the atmosphere, chemical processes, and, finally, the climate.

## Conclusion

The main result of this review can be formulated very shortly: the now available observations only schematically represent the wide variety of the properties and the space-time variability of the global aerosol, thus significantly restricting our capabilities of obtaining the needed information even through numerical simulation.

## References

1. M.Yu. Arshinov and B.D. Belan, *Atmos. Oceanic Opt.* **13**, No. 11, 909\$916 (2000).
2. A.A. Grigor'ev and K.Ya. Kondratyev, *Ecological Disasters* (Scientific Center of RAS, St. Petersburg, 2001), 350 pp.
3. A.P. Il'in, A.A. Gromov, and E.M. Popenko, *Atmos. Oceanic Opt.* **13**, No. 11, 917\$920 (2000).
4. A.S. Kozlov, A.N. Ankilov, A.M. Baklanov, A.L. Vlasenko, S.I. Eremenko, and S.B. Malyshkin, *Atmos. Oceanic Opt.* **13**, Nos. 6\$7, 617\$619 (2000).
5. K.Ya. Kondratyev, O.B. Vasil'ev, O.S. Ivlev, G.A. Nikol'skii, and O.I. Smoktii, *Effect of Aerosol on Radiative Transfer: Possible Climatic Consequences* (Leningrad State University Publishing House, Leningrad, 1973), 266 pp.
6. K.Ya. Kondratyev, N.I. Moskalenko, and D.V. Pozdnyakov, *Atmospheric Aerosol* (Gidrometeoizdat, Leningrad, 1983), 224 pp.
7. K.Ya. Kondratyev, ed., *Aerosol and Climate* (Gidrometeoizdat, Leningrad, 1991), 542 pp.
8. K.Ya. Kondratyev, *Atmos. Oceanic Opt.* **14**, No. 3, 153\$160 (2001).
9. K.Ya. Kondratyev and K.S. Demirchan, *Vestn. RAN* **71**, No. 11 (2001).
- 9=. K.P. Koutsenogii and P.K. Koutsenogii, *Sib. Ekol. Zh.* **7**, No. 1, 11\$20 (2000).
10. V.A. Obolkin, V.L. Potemkin, and T.V. Khodzher, *Atmos. Oceanic Opt.* **11**, No. 6, 547\$549 (1998).
11. V.V. Penenko and M.V. Panchenko, *Atmos. Oceanic Opt.* **13**, Nos. 6\$7, 647\$652 (2000).
12. E.A. Romankevich and A.A. Vetrov, *Carbon Cycle in Russian Arctic Seas* (Nauka, Moscow, 2001), 303 pp.
13. O.G. Khutorova, G.M. Tepkin, and A.F. Latypov, *Atmos. Oceanic Opt.* **13**, Nos. 6\$7, 631\$634 (2000).
14. M.O. Andrea, J. Fishman, and J. Lindesay, *J. Geophys. Res. D* **101**, No. 19, 23519\$23520 (1996).
15. M.C. Barth and A.T. Church, *J. Geophys. Res. D* **104**, No. 23, 30231\$30240 (1999).
16. M.C. Barth, P.J. Rasch, J.T. Kiehl, C.M. Benkovitz, and S.E. Schwartz, *J. Geophys. Res. D* **105**, No. 1, 1387\$1416 (2000).
17. T.S. Bates, B.J. Huebert, J.L. Gras, F.B. Criffiths, and P.A. Durkee, *J. Geophys. Res. D* **103**, No. 13, 16297\$16318 (1998).
18. T.S. Bates, *J. Geophys. Res. D* **104**, No. 17, 21645\$21647 (1999).
- 18a. O.H. Berg, E. Swietlicki, and R. Krejci, *J. Geophys. Res. D* **103**, No. 13, 16535\$16545 (1988).
19. H. Berresheim, J.W. Huey, R.P. Thorn, F.L. Eisele, D.J. Tanner, and A. Jefferson, *J. Geophys. Res. D* **103**, No. 1, 1629\$1637 (1998).
20. W. Birmili and A. Wiedensohler, *Geophys. Res. Lett.* **27**, No. 20, 3325\$3328 (2000).
21. G. Buzoruz, U. Rannik, J.M. Makela, P. Keronen, T. Vesala, and M. Kulmala, *J. Geophys. Res. D* **105**, No. 15, 19905\$19916 (2000).
22. R. Cappellato, N.E. Peters, and T.P. Meyers, *Water, Air, and Soil Pollut.* **103**, Nos. 1\$4, 151\$171 (1998).
23. M. Chin, R.B. Rood, S.-J. Lin, J.-F. Muller, and A.M. Thompson, *J. Geophys. Res. D* **105**, No. 20, 24671\$24688 (2000).
24. M. Chin, D.L. Savoie, B.J. Huebert, A.R. Bandy, D.C. Thornton, T.S. Bates, P.K. Quinn, E.S. Saltzman, and W.J. De Bruyn, *J. Geophys. Res. D* **105**, No. 20, 24689\$24712 (2000).
- 24a. A.R. Chughthai, M.I. Miller, D.M. Smith, and J.R. Pitts, *J. Atmos. Chem.* **34**, No. 2, 259\$279 (1999).
25. W.D. Collins, P.J. Rasch, B.E. Eaton, B.V. Khattatov, and J.-F. Lamarque, *J. Geophys. Res. D* **106**, No. 7, 7313\$7336 (2001).
26. D. Davis, G. Chen, P. Kasibhatla, A. Jefferson, D. Tanner, F. Eisele, D. Lenschow, W. Neff, and H. Berresheim, *J. Geophys. Res. D* **103**, No. 1, 1657\$1678 (1998).
27. J.E. Dibb, R.W. Talbot, E.M. Scheuer, D.R. Blake, N.S. Blake, G.L. Gregory, G.W. Sachse, and D.C. Thornton, *J. Geophys. Res. D* **104**, No. 5, 5785\$5800 (1999).
28. G. Feingold, S.M. Kreidenweis, B. Stevens, and W.R. Cotton, *J. Geophys. Res. D* **101**, No. 16, 21391\$21402 (1996).
29. G. Feingold and S. Kreidenweis, *J. Geophys. Res. D* **105**, No. 19, 24351\$24362 (2000).
30. J.W. Fitzgerald, W.A. Hoppel, and F. Gelbard, *J. Geophys. Res. D* **103**, No. 13, 16085\$16102 (1998).
31. J.W. Fitzgerald, J.S. Marti, W.A. Hoppel, G.M. Frick, and F. Gelbard, *J. Geophys. Res. D* **103**, No. 13, 16103\$16117 (1998).
32. W. Guelle, Y.J. Balkanski, M. Schultz, B. Marticorena, G. Bergametti, C. Moulin, R. Arimoto, and K.D. Perry, *J. Geophys. Res. D* **105**, No. 2, 1997\$2012 (2000).
33. G.H. Güllü, I. Olmez, S. Aygün, and B. Tuncel, *J. Geophys. Res. D* **103**, No. 17, 21943\$21954 (1998).
34. R.M. Harrison, J.L. Grenfell, N. Savage, A. Allen, K.C. Clementshaw, S. Penkett, C.N. Hewitt, and B. Davison, *J. Geophys. Res. D* **105**, No. 14, 17819\$17832 (2000).
35. P.V. Hobbs, *IGACTiv. News Lett.*, No. 11, 3\$5 (1998).
36. J.T. Houghton, in: *Proc. of the SOLSPA Conf.*, Tenerife, 25\$29 Sept., 2000, ESA SP ISSN 0379\$6566, No. 463, (Nardwijk, 2000), pp. 255\$259.
37. S. Huang, K.A. Rahn, R. Arimoto, W.C. Graurtein, and K.K. Turekian, *J. Geophys. Res. D* **104**, No. 23, 30309\$30317 (1999).
38. B.J. Huebert, S.G. Howell, L. Zhuang, J.A. Heath, M.R. Litchy, D.J. Wylie, J.L. Kreidler-Moss, S. Cöppicus, and J.E. Pfeiffer, *J. Geophys. Res. D* **103**, No. 13, 16493\$16509 (1998).
39. J.T. Houghton et al., eds., *IPCC, Climate Change 2001: The Scientific Basis* (Cambridge University Press, 2001), 881 pp.
40. A.M. Johansen, R.L. Siefert, and M.R. Hoffman, *J. Geophys. Res. D* **105**, No. 12, 15277\$15312 (2000).
41. M. Kanakidou, K. Tsigaridis, F.J. Dentener, and P.J. Crutzen, *J. Geophys. Res. D* **105**, No. 7, 9243\$9254 (2000).
42. N. Kaneyasu and S. Murayama, *J. Geophys. Res. D* **105**, No. 15, 19881\$19890 (2000).
43. B. Kärcher, R.P. Turco, E. Yu, M.Y. Danilin, D.K. Weisenstein, R.C. Miake-Lye, and R. Busen, *J. Geophys. Res. D* **105**, No. 24, 29379\$29386 (2000).

44. V.-M. Kerminen, R.E. Hillamo, T. Mäkelä, J.-L. Saffrezo, and W. Maenhut, *J. Geophys. Res. D* **103**, No. 5, 5661\$5670 (1998).
45. K.Ya. Kondratyev, *Climate Shocks: Natural and Anthropogenic* (John Wiley & Sons, New York, 1988), 296 pp.
46. K.Ya. Kondratyev and I. Galindo, *Volcanic Activity and Climate* (A. Deepak Publ., Hampton, VA, 1997), 382 pp.
47. K.Ya. Kondratyev, *Multidimensional Global Change* (Wiley/PRAXIS, Chichester, U.K., 1998), 761 pp.
48. K.Ya. Kondratyev, *Climate Effects of Aerosols and Clouds* (Springer/PRAXIS, Chichester, U.K., 1999), 264 pp.
49. U. Krischke, R. Staubes, T. Brauers, M. Gautrois, J. Burkert, D. Stobæner, and W. Jaeschke, *J. Geophys. Res. D* **105**, No. 11, 14413\$14422 (2000).
50. D. Lavoué, C. Lioussé, H. Cachier, B. Stocks, and J.G. Goldammer, *J. Geophys. Res. D* **105**, No. 22, 26871\$26890 (2000).
51. K. Li-Jones and J.M. Prospero, *J. Geophys. Res. D* **103**, No. 13, 16073\$16084 (1998).
52. C. Mari, K. Suhre, R. Rosset, T.S. Bates, B.J. Huebert, A.R. Bandy, D.C. Thornton, and S. Bussinger, *J. Geophys. Res. D* **104**, No. 17, 21733\$21749 (1999).
53. H. Maring, D.L. Savoie, M.A. Izaguirre, C. McCormick, R. Arimoto, J.M. Prospero, and C. Pilnis, *J. Geophys. Res. D* **105**, No. 11, 14677\$14700 (2000).
54. E. Mészáros, *Fundamentals of Atmospheric Aerosol Chemistry* (Akadémiai Kiadó, Budapest, 1999), 308 pp.
- 54a. E. Mészáros and A. Molnar, *Időjárás* **105**, No. 2, 63\$80 (2001).
55. M. Mishchenko, J. Penner, and D. Anderson, *GEWEX News* **10**, No. 4, 6 (2000).
56. K.K. Moorthy and S.K. Satheesh, *Quart. J. Roy. Meteorol. Soc. Part A* **126**, No. 562, 81\$110 (2000).
57. D.M. Murphy, J.R. Anderson, P.K. Quinn, L.M. McInnes, F.J. Brechtel, S.M. Kreidenweis, A.M. Middlebrook, M. Pösfai, D.S. Thomson, and P.R. Buseck, *Nature* **392**, No. 6671, 62\$65 (1998).
58. R.E. Newell and M.J. Evans, *Geophys. Res. Lett.* **27**, No. 16, 2500\$2512 (2000).
59. C.D. O'Dowd, M. Geever, M.K. Hill, M.H. Smith, and S.G. Jennings, *Geophys. Res. Lett.* **25**, No. 10, 1661\$1664 (1998).
60. C.D. O'Dowd, E. Becker, J.M. Mäkelä, and M. Kulmala, *Boreal Environ. Res.* **5**, No. 4, 337\$348 (2000).
61. J. Park and S.Y. Cho, *Atmos. Environ.* **32**, No. 16, 2745\$2756 (1998).
62. S.J. Piketh, H.J. Annegam, and P.D. Tyson, *J. Geophys. Res. D* **104**, No. 1, 1597\$1607 (1999).
63. L. Pirjola, A. Laaksonen, and M. Kulmala, *J. Geophys. Res. D* **103**, No. 7, 8309\$8321 (1998).
64. A.V. Polissar, P.K. Hopke, P. Pantero, W.C. Malm, and J.F. Sisler, *J. Geophys. Res. D* **103**, No. 15, 19045\$19057 (1998).
65. A.V. Polissar, P.K. Hopke, W.C. Malm, and J.F. Sisler, *J. Geophys. Res. D* **103**, No. 15, 19035\$19044 (1998).
66. M. Posfai, J.R. Anderson, P.R. Buseck, and H. Sievering, *J. Geophys. Res. D* **104**, No. 17, 21685\$21694 (1999).
67. C.E. Randall, R.M. Bevilacqua, J.D. Lumple, K.W. Hoppel, D.W. Rusch, and E.P. Shettle, *J. Geophys. Res. D* **105**, No. 3, 3929\$3942 (2000).
68. P.J. Rasch, W.D. Collins, and B.E. Eaton, *J. Geophys. Res. D* **106**, No. 7, 7337\$7355 (2001).
69. K. Restad, S.A. Isaksen, and T.K. Bernsten, *Atmos. Environ.* **32**, No. 20, 3593\$3609 (1998).
70. M. Reus, J. Strom, J. Curtius, L. Pirjola, E. Vignati, F. Arnold, H.C. Hansson, M. Kulmala, J. Lelievre, and F. Raes, *J. Geophys. Res. D* **105**, No. 20, 24751\$24762 (2000).
71. J. Rosen, S. Young, J. Laby, N. Kjome, and J. Gras, *J. Geophys. Res. D* **105**, No. 14, 17833\$17842 (2000).
72. P.J. Rasch, M.C. Barth, J.T. Kiehl, S.E. Schwartz, and C.M. Benkovitz, *J. Geophys. Res. D* **105**, No. 1, 1367\$1386 (2000).
73. S.K. Satheesh, V. Ramanathan, X. Li-Jones, J.M. Lobert, I.A. Podgorny, J.M. Prospero, B.N. Holben, and N.G. Loeb, *J. Geophys. Res. D* **104**, No. 22, 27421\$27440 (1999).
74. J. Savarino and M. Legrand, *J. Geophys. Res. D* **103**, No. 7, 8267\$8279 (1998).
75. J. Savarino, C.C.W. Lee, and M.H. Thiemens, *J. Geophys. Res. D* **105**, No. 23, 29079\$29088 (2000).
76. T. Takemura, H. Okamoto, Y. Maruyama, A. Numaguti, A. Higurashi, and T. Nakajima, *J. Geophys. Res. D* **105**, No. 14, 17853\$17874 (2000).
77. Tegen, P. Hollrig, M. Chin, I. Fung, D. Jacob, and J. Penner, *J. Geophys. Res. D* **102**, No. 20, 23895\$23915 (1997).
78. Tegen, D. Koch, A.A. Lacis, and M. Sato, *J. Geophys. Res. D* **105**, No. 22, 26971\$26990 (2000).
79. K. Teinilä, V.-M. Kerminen, and R. Hillamo, *J. Geophys. Res. D* **105**, No. 3, 3893\$3905 (2000).
80. P. Wählin, in: *Chemical Exchange Between the Atmosphere and Polar Snow*, ed. by E.W. Wolff and R.C. Baler, NATO ASI Series I (Springer-Verlag, Berlin; Heidelberg, 1996), Vol. 43, pp. 131\$143.
81. E.W. Wolff and H. Cachier, *J. Geophys. Res. D* **103**, No. 9, 11033\$11042 (1998).
82. S. Wurzker, T.G. Reisin, and Z. Levin, *J. Geophys. Res. D* **105**, No. 4, 4501\$4512 (2000).